

Unclassified

SECURITY CLASSIFICATION OF THIS PAGE (When Data Entered)

①

5

AD A091329

17

REPORT DOCUMENTATION PAGE		READ INSTRUCTIONS BEFORE COMPLETING FORM
1. REPORT NUMBER AFGL-TR-80-0303	2. GOVT ACCESSION NO. AD-A092	3. RECIPIENT'S CATALOG NUMBER 339
4. TITLE (and Subtitle) IMPULSIVE PHASE OF SOLAR FLARES		5. TYPE OF REPORT & PERIOD COVERED Scientific. Interim.
7. AUTHOR(s) Sharad R./Kane U./Feldman M. R. Kundu C. J./Crannell A./Gabriel C. Matzler D./Datlowe H. S. Hudson D. Neidig		8. CONTRACT OR GRANT NUMBER(s) 11441
9. PERFORMING ORGANIZATION NAME AND ADDRESS Air Force Geophysics Laboratory (PHS) Hanscom AFB Massachusetts 01731		10. PROGRAM ELEMENT, PROJECT, TASK AREA & WORK UNIT NUMBERS 2311G310
11. CONTROLLING OFFICE NAME AND ADDRESS Air Force Geophysics Laboratory (PHS) Hanscom AFB Massachusetts 01731		12. REPORT DATE 2 October 1980
14. MONITORING AGENCY NAME & ADDRESS (if different from Controlling Office)		13. NUMBER OF PAGES 43
		15. SECURITY CLASS. (of this report) Unclassified
		15a. DECLASSIFICATION/DOWNGRADING SCHEDULE

16. DISTRIBUTION STATEMENT (of this Report)
~~Approved for public release; distribution unlimited~~

DTIC ELECTED
NOV 6 1980

17. DISTRIBUTION STATEMENT (of the abstract entered in Block 20, if different from Report)
B

18. SUPPLEMENTARY NOTES Reprinted from Solar Flares, A Monograph from Skylab Solar Workshop II (Ed. P. A. Sturrock), Colorado Associated University Press, Boulder, CO, pp. 187-229, June, 1980

19. KEY WORDS (Continue on reverse side if necessary and identify by block number)

Solar flares
Particle acceleration
X-rays

THIS DOCUMENT IS BEST QUALITY PRACTICABLE.
THE COPY FURNISHED TO YOU CONTAINED A
SIGNIFICANT NUMBER OF PAGES WHICH DO NOT
REPRODUCE LEGIBLY

20. ABSTRACT (Continue on reverse side if necessary and identify by block number)

A review of hard x-ray, microwave, and optical observations of the impulsive phase of solar flares provides substantial evidence for non-thermal electrons as the basic source of energy in the early stages of the flare. Direct thermal input, however, can not be ruled out. The basic observational data are used to assess a self-consistent flare model and to determine what future observations will be required in order to model the flare in more detail.

Block 7: Cont'd: V. Petrosian, N. R. Sheeley, Jr.

DD FORM 1 JAN 73 1473

Unclassified 4-09578 slr
SECURITY CLASSIFICATION OF THIS PAGE (When Data Entered)

DISCLAIMER NOTICE

**THIS DOCUMENT IS BEST QUALITY
PRACTICABLE. THE COPY FURNISHED
TO DTIC CONTAINED A SIGNIFICANT
NUMBER OF PAGES WHICH DO NOT
REPRODUCE LEGIBLY.**

5. IMPULSIVE PHASE OF SOLAR FLARES

Shrad R. Kane; C. J. Crannell, D. Datlowe, U. Feldman, A. Gabriel, H. S. Hudson, M. R. Kundu, C. Mätzler, D. Neidig, V. Petrosian, and N. R. Sheeley, Jr.

5.1 INTRODUCTION

The impulsive phase of a solar flare is characterized by short duration (10-1000 s) bursts of impulsive hard X-ray, extreme ultraviolet (EUV), optical, and radio emission. A large part of the work on the impulsive phase has so far been concentrated on establishing quantitatively the interrelationships among the various emissions, the temporal evolution of these relationships, and modeling of the emission sources. Because of the limited temporal and spatial resolution of most of the past observations, only an approximate, average description of the impulsive phase has been achieved. It is clear, however, that in spite of its short duration, energetically the impulsive phase is probably the most important phase of a solar flare.

During the past decade, perhaps the most significant advance in the understanding of solar flares came from studies of energetic particles, especially electrons. These particles, which were previously considered as only one of the many secondary effects in solar flares, have been found to play a central role in the flare energetics. This is particularly true for the impulsive phase, where most of the released energy seems to appear initially in the form of energetic electrons which directly or indirectly provide the necessary energy to other flare phenomena. The impulsive phase has thus assumed a new significance and is expected to provide major clues to the nature of particle acceleration processes and therefore to the basic flare mechanisms.

This review of our present understanding of the impulsive phase begins with a brief background and an identification of the key questions related to this phenomenon. These are followed by an analysis of the various impulsive emissions and the models proposed to explain their origin. Finally, we consider the role of the impulsive phase in the overall flare process and suggest future observational and theoretical studies which will bring us closer to an understanding of solar flares.

5.2 BACKGROUND, KEY QUESTIONS, AND APPROACH

A solar flare, in general, produces a variety of electromagnetic and particle radiations. An example is shown in Figure 5.1. The time-intensity profile of the observed radiation depends on a number of factors. Some of these factors are:

1. Type of radiation (electromagnetic, particle)
2. Spectral characteristics (frequency or energy, line or continuum)

80 10 14 044

3. Spatial resolution of the instrumentation
4. Magnitude of the flare
5. Location of the flare on the solar disk
6. Flare activity preceding the flare being observed.

In addition, there is an apparently random variation in several less-known factors (e.g., magnetic field topology) from one flare to another. In spite of these variations, the gross features of the time-intensity profile of a solar flare can be divided into three principal phases, viz. precursor phase, impulsive phase, and gradual phase (cf. Fig. 1 of Kane, 1974a).

In this chapter, we are primarily concerned with the impulsive phase. The principal characteristics of this phase have been reviewed extensively (cf. Kundu, 1965; Kane, 1974a). The impulsive phase lasts for about 10 to a few hundred seconds, depending on the magnitude of the flare, and is characterized by the most rapid variations in the radiation flux during the lifetime of the flare. The variations, are most prominent at hard X-ray, EUV, and some optical and radio wavelengths. The production of hard X-rays and impulsive radio emissions, such as microwave and Type III radio bursts, indicate the presence of energetic (about 10 to a few hundred keV) electrons in the flare region. Such energetic electrons have also been observed in interplanetary space following solar flares. When the propagation delay from the sun to the point of observation is taken into account, the observations of these electrons indicate that they are released during the impulsive phase of the flare (Arnoldy *et al.*, 1968; Lin, 1970; Lin and Hudson, 1971). On the other hand, the measurements of the flare γ -ray emission (Cupp *et al.*, 1975; Talon *et al.*, 1975) and interplanetary solar protons indicate that energetic protons are probably produced after the impulsive phase (Bai and Ramaty, 1976). Thus, acceleration of ~ 10 to a few hundred keV electrons, rather than high-energy protons, is the most characteristic feature of the impulsive phase.

When the total kinetic energy of the energetic electrons in the flare region is estimated from the hard X-ray observations, it is found that the electron energy may be comparable to the total energy released during the impulsive phase. Therefore, the impulsive phase represents a process in which a large fraction of the total energy released during a flare appears in the form of energetic electrons. The exact value of this fraction, also called "acceleration efficiency," depends on the assumed model of the hard X-ray source and is therefore not known at the present time. The acceleration efficiency probably varies from one flare to another. In some flares it seems to reach a value as high as about 100%.

The distribution of energetic electrons and their total energy are deduced from the hard X-ray observations. The exact relationship between the hard X-ray spectrum emitted by the source and the electron spectrum which generates the X-rays depends on the details of the model. Assuming bremsstrahlung as the radiation process, two extreme situations could occur, viz., "thick-target" and "thin-target" bremsstrahlung. Also, the electron spectrum could be "thermal" or "nonthermal." A thick-target model and/or a thermal electron spectrum places, in general, a lower energy and number requirement on the electrons. Accurate measurement and interpretation of the hard X-ray emission are therefore vital for an understanding of the flare energetics as well as the basic physical processes governing particle acceleration in solar flares.

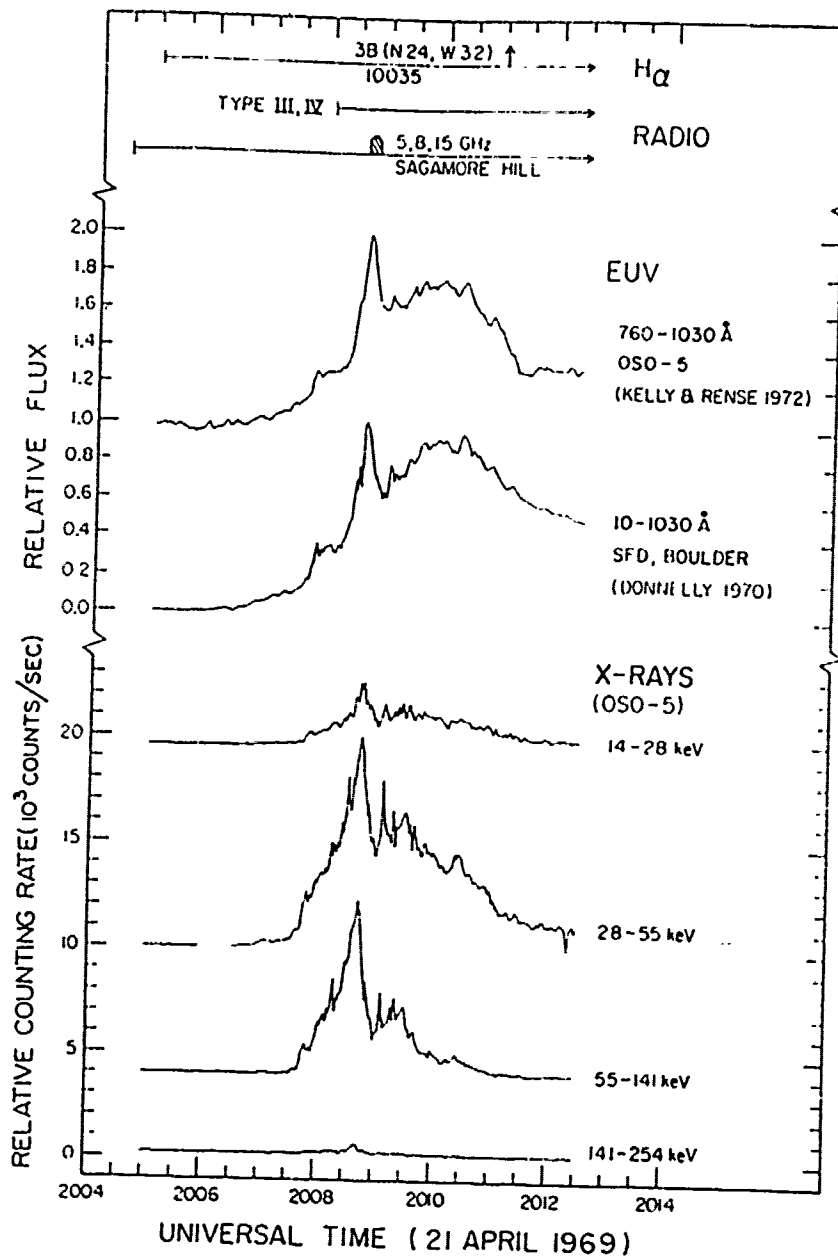


Fig. 5.1 An example of impulsive EUV and hard X-ray emissions in a solar flare. In this event, the impulsive phase occurred from about 2007.7 UT to 2009.0 UT. The impulsive phase was preceded by a low level gradual emission (precursor) and was followed by a relatively intense gradual emission (gradual phase). Notice the excellent agreement between the EUV emission observed by the broadband EUV spectrometer aboard the OSO-5 satellite (Kelly and Rense, 1972) and the EUV emission deduced from the ground based measurements of the Sudden Frequency Deviation (SFD) an ionospheric effect (Kane, et al. 1978).

SEARCHED

SERIALIZED

INDEXED

FILED

APR 21 1969

FBI - WASH DC

In this chapter, we consider the following key questions regarding the impulsive phase:

1. Is the distribution of energetic electrons thermal or non-thermal?
2. Do the energetic particles (electrons), produced during the impulsive phase, provide the energy for the whole flare?
3. Among the models of the impulsive phase suggested so far, which ones are most consistent with observations?

In order to answer the above key questions, it is necessary to know the spectrum of the energetic electrons and their total energy e_e , as well as the total energy e_r radiated by the flare region during the impulsive phase. The energy ($e_e - e_r$) available for the remainder of the flare can then be evaluated. It is also necessary to know the spectral energy distribution of the impulsive radiation and its temporal and spatial variation to test the validity of the impulsive-phase models. Specifically, our approach to obtain the answers to the three key questions consists of the following:

1. Critical review of the impulsive hard X-ray and microwave burst observations and their interpretation in terms of the distribution of energetic electrons.
2. Review of the observations of the impulsive EUV and optical radiations, which give a lower limit for the total energy released during the impulsive phase.
3. Analysis of the measurements made during the Skylab observation period, particularly those in which soft X-ray and EUV images were obtained with relatively high time resolution at or near the time of the impulsive phase.
4. Evaluation of the models proposed so far for the impulsive phase in light of the above review and analysis.

In the process of finding answers to the key questions, we hope to learn what future observations and theoretical studies are most likely to lead to a more complete understanding of the solar flare phenomena.

5.3 HARD X-RAY EMISSION

The initial observations of impulsive hard X-ray bursts by Peterson and Winckler (1959), Anderson and Winckler (1962) and others, were followed by a sequence of satellite experiments with better time and energy resolution, resulting in observations of many hundreds of events. Table 5.1 lists the important experiments and their instrumental parameters. The observational characteristics of the impulsive hard X-ray emission include its time variability, spectral distribution, polarization, directionality, and location of emission. However, at this time adequate observations of only the first two of these categories are available. We will therefore confine our discussion primarily to the following three observational characteristics: (1) true spectral distribution; (2) time variation of the spectrum during a flare; and (3) organization of the impulsive hard X-ray bursts into distinguishable classes. Clearly, the observations with highest available time resolution (about 1 s) are to be

Accession For	
NTIS GRA&I	<input checked="" type="checkbox"/>
DTIC TAB	<input type="checkbox"/>
Unannounced	<input type="checkbox"/>
Justification _____	
By _____	
Distribution/	
Availability Codes	
Dist	Avail and/or Special
A	29/21 <i>23</i>

TABLE 5.1
IMPORTANT SATELLITE OBSERVATIONS OF HARD SOLAR X-RAYS

Spacecraft	Dates	Detector Type	Area (cm ²)	Time Res. (s)	Window material thickness (cm)	$E_{1/2}$ (eV)	$\Delta E_{3\sigma}$ range (eV)	Energy Res. (WFSM - 30 keV) (eV)	Reference
OSO-1	Mar. 1962- May 1963	NaI(Tl)	3.8	20	Al	0.08	19	0.2-4	80 ^a Frost (1962)
OGO-1, OGO-3	Sept. 1964- Dec. 1967	Ion. ch.	250	1-10	Al	0.089	19	≥ 1	39 ^d Arnoldy et al (1968)
OSO-3	Mar. 1967- June 1968	NaI(Tl)	9.6	15	Be	0.051	4.1	1-4	11 Hudson et al. (1969)
OGO-5	Mar. 1968- June 1971	NaI(Tl)	9.6	≤ 2.3	Be	0.051	4.1	0.03-4	16 Kane and Anderson (1970)
OSO-5	Jan. 1969- Mar. 1971	CsI(Na)	54 (5,4) ^b	1.8	Al ^b	0.054	> 16	0.1-30	33 Cannell et al (1973)
OSO-6	Aug. 1969- Mar. 1972	NaI(Tl)	5.1 (0.2) ^c	6.1	Al	0.015	11.5	0.5-3	22 Barnard et al (1973)
OSO-7	Oct. 1971- June 1973	NaI(Tl)	9.6 (2,4) ^c	10.2	Al	0.015	12	0.02-6	6,5 Dobrow et al. (1974)
TD-1A	Mar. 1972- May 1974	CsI(Na)	5	1.2	Si ^b	0.072	25	0.3-1.50	8,5 Hosokawa et al (1976)
ISEE-3	Aug. 1978- present	NaI(Tl)	22	0.1-0.5	Mg ^b	0.076	20	≥ 0.03	8,5 Kane and Anderson (1975)

^a No Energy Discrimination.

^b Additional absorber present.

^c Effective Area averaged over one spin period of the spacecraft.

^d $E_{1/2}$ represents the X-ray energy corresponding to 50% transmission.

^e $\Delta E_{3\sigma}$ = Differential photon flux (photons cm⁻² s⁻¹ keV⁻¹) at 30 keV.

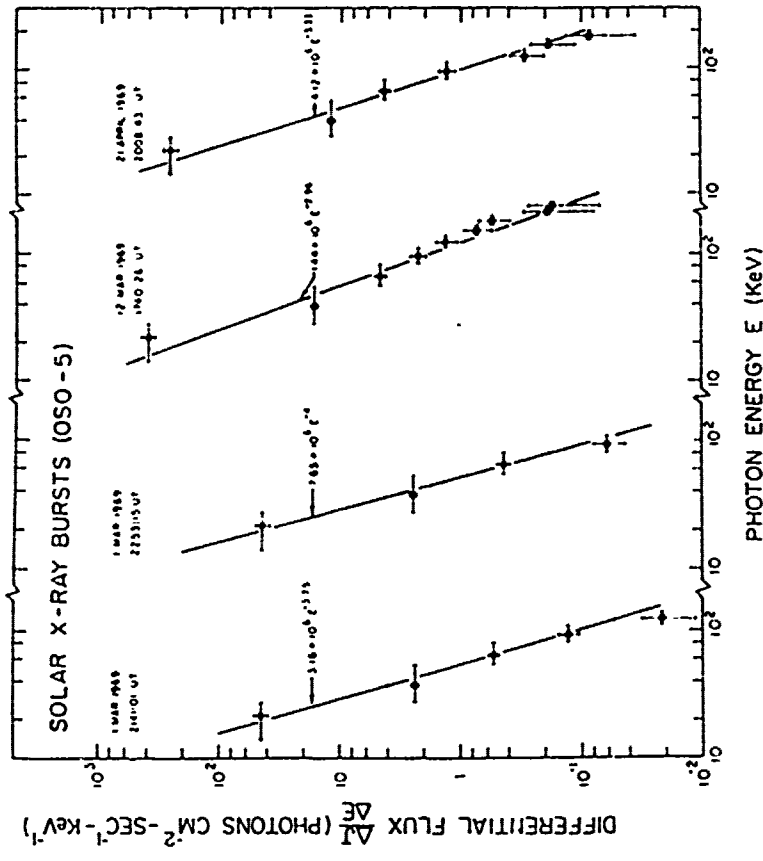


Fig. 5.2 Examples of hard X-ray spectra at the peaks of the impulsive bursts, measured with the OSO-5. The straight lines, which represent power-law spectra ($\sim E^{-\gamma}$ photons $\text{cm}^{-2} \text{ s}^{-1} \text{ keV}^{-1}$), are shown for comparison. It can be seen that the observed X-ray spectra are consistent with a power law in 15-80 keV range, with some steepening at higher energies (Kane, et al., 1978).

emphasized. Moreover, it is important to note that the interpretation of the observations depends, in general, on the detailed characteristics of the hard X-ray source, including the assumed X-ray emission mechanisms, source structure, and propagation conditions. These aspects of the interpretation will be discussed in Section 5.8.

5.3.1. Spectrum

Examples of hard X-ray spectra at the peak of impulsive emission are shown in Fig. 5.2. The spectra fall off steeply above about 10 keV and can be characterized by a power-law fit ($\sim (h\nu)^{-\gamma}$ photons $\text{cm}^{-2} \text{ s}^{-1} \text{ keV}^{-1}$) over 10–80 keV range, with $\gamma \geq 2.5$. Thus, there is an upper limit to the hardness of the impulsive X-ray spectrum and, hence, that of the electron spectrum in the X-ray source (Kane, 1971). It has also become clear that a second phase of *gradual* hard X-ray emission occurs during major flares (Frost and Dennis, 1971; Hoyng et al., 1976; Hudson, 1978). Hoyng et al. (1976) describe these events as "extended bursts." We do not have sufficient observations to prove the existence of this second type of solar hard X-ray emission strictly from some distribution in parameter space, but the characteristics of the limited group (~ 5 flares) of gradual hard X-ray bursts seem to distinguish them clearly enough. We discuss only the impulsive bursts here.

The spectrometers used to date (Table 5.1) have not had sufficient spectral resolution to describe the X-ray spectrum in much detail. For most analyses this has forced the adoption of simple two-parameter fits (power law or exponential, nominally corresponding to nonthermal and thermal bremsstrahlung, respectively). Going beyond this simple spectral modeling, most of the impulsive-phase spectra measured later than OSO-3 (Hudson et al., 1969) show a steepening with increasing energy as compared to a single power law (Frost, 1969; Kane and Anderson, 1970; Frost and Dennis, 1971; Hoyng et al., 1976; Eicam, 1978). The steepening may result in a better two-parameter fit to an exponential law, as can be seen from Fig. 5.3. The spectra may also have further complexity, but the data probably do not have high enough quality to resolve it.

It is important to have a statistical description of hard X-ray occurrence in flares. Given power-law spectral fits of the form $J = A_{20} (h\nu/20)^{-\gamma}$ photons $(\text{cm}^2 \text{ s keV})^{-1}$, where A_{20} is the photon flux at 20 keV, we need to know the exact distributions of spectral index γ and flux A_{20} at the maxima of different X-ray bursts and also their cross-correlation, for a set of well-observed flares. Unfortunately, the instruments used for observations to date have not given uniformly good coverage of the (γ, A_{20}) parameter space. Furthermore, differing energy resolution, the coupling of parameters in this nonlinear fitting, and other systematic effects make intercomparison of different experiments difficult. Still worse, the extreme dynamic range in the hard X-ray flux presented by the sun has made different instruments sensitive to almost mutually exclusive domains of parameter space.

For X-ray measurements with about 10-s time resolution, the most complete statistical analysis has come from the OSO-7 data (Datlowe, 1975; Datlowe et al., 1974, 1979). These data show, for hard X-ray bursts associated mainly with subflares, that $2 < \gamma < 7$ for the spectra at peak flux (123 events), with a median $\gamma = 4.0$. Little correlation existed between A_{20} , the peak flux at 20 keV, and γ over the OSO-7 dynamic range. A similar result was reported earlier by Kane

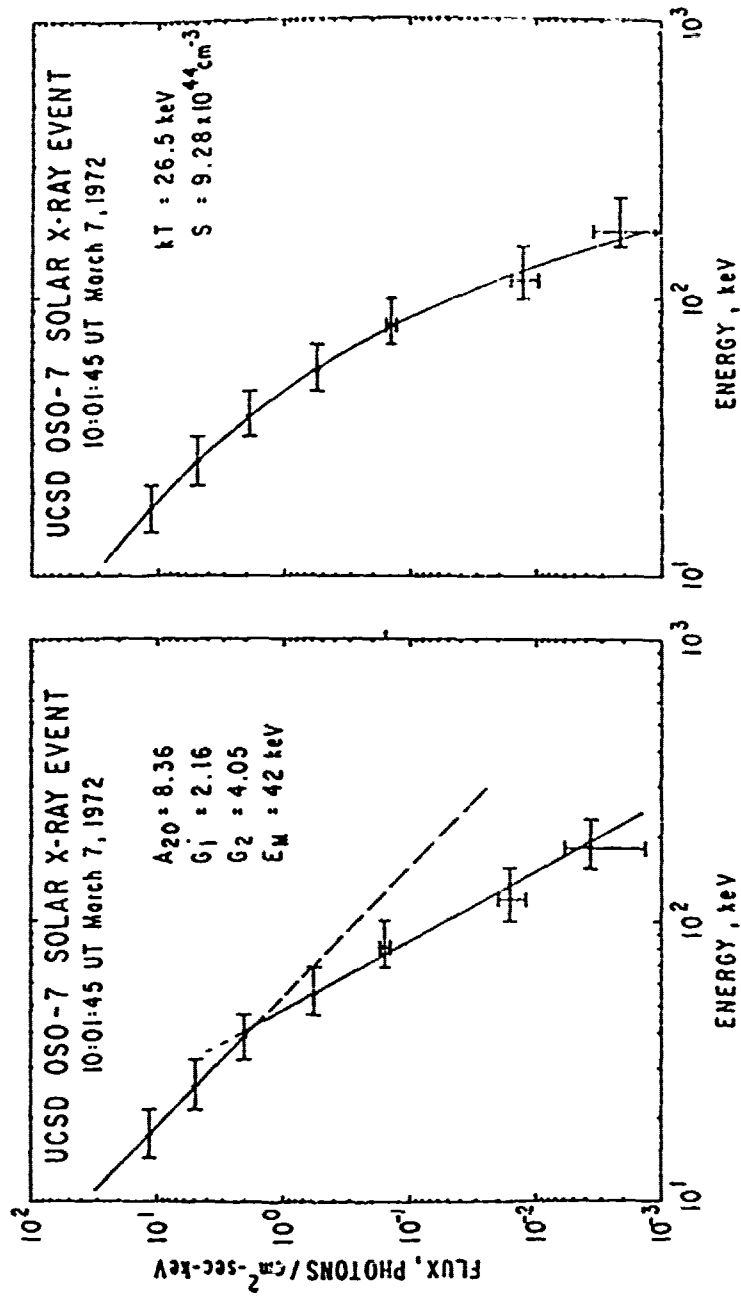


Fig. 5.3 Power-law ($\sim E^{-\gamma}$) and thermal spectral fits to an impulsive hard X-ray burst observed with the OSO-7 satellite. The power-law fit (left) requires $\gamma = 2.16$ in 10–42 keV range and $\tau = 4.05$ in 42–200 keV range. A thermal fit (right) can be obtained with a single temperature $kT = 26.5$ keV (Elean, 1978).

(1974b) for the OGO-5 measurements, which had a higher time resolution but smaller dynamic range. However, a few large events, such as the August 1972 flares, observed with TD-1A (Hoing *et al.*, 1976) show appreciably harder spectra.

A thermal interpretation of the hard X-ray spectrum gives $5 < kT < 60$ keV, with "emission measure" in the range of $10^{44} - 10^{45}$ cm³ (Crannell *et al.*, 1978; Lican, 1978). The weak dependence of γ on the intensity of a flare implies that the peak temperature of a thermal hard X-ray burst does not depend strongly upon total flare energy.

A power-law spectral fit implicitly contains a third parameter, a low-energy cutoff that prevents the total energy from diverging. If the power law does fit better than the exponential law, soft X-ray measurements must determine this cutoff energy. Even without the presence of the very intense soft X-ray component, the cutoff energy represents a real challenge to the experimentalist: a perfectly sharp cutoff in the electron spectrum at E_0 results in only a gradual roll-off in the bremsstrahlung spectrum at lower energies.

Kahler and Kreplin (1971) reported nonthermal emission at $h\nu \sim 3$ keV from OGO-5 observations. This conclusion rests more on the time profiles than on the spectral evidence and should therefore be repeated with better spectral resolution. Peterson *et al.* (1973) showed a spectrum with a power law extending downward to 5 keV; however, this burst did not show any impulsive emission at ~ 5 keV and seemed to be unique among ~ 400 hard X-ray bursts detected by OSO-7.

Direct X-ray measurements probably cannot adequately define a low-energy cutoff without much higher spectral resolution, temporal resolution, and dynamic range. Good spatial resolution would help enormously in reducing the soft X-ray background against which we measure the impulsive-phase hard X-ray spectrum.

5.3.2. Time Variation

The hard X-ray emission may fluctuate rapidly during the impulsive phase. An example is shown in Fig. 5.4. Anderson and Mahoney (1974) and Hurley and Duprat (1977) observed e-folding times of about 1.0 s at an effective energy of about 40 keV, somewhat shorter times than those reported by Kane and Anderson (1970). Frost (1969) and Crannell *et al.* (1978) found unresolved events at 1.8 s time resolution. The properties of "elementary flare bursts," which represent short-lived bursts in a large flare (Van Beek *et al.*, 1974; de Jager and de Jonge, 1978) are not inconsistent with these observations. Further progress requires a thorough statistical analysis of high time-resolution observations.

Quasi-periodic structures with periods of about 30 s have been observed in some multispiked X-ray bursts (Parks and Winckler, 1969; Frost, 1969). Petrosian (in collaboration with B. Lippa) has analyzed multispiked X-ray bursts observed with OSO-5. Strict periodicities do not exist, but quasi-periodic modulations have been found for a majority of the bursts analyzed. Periods ranging from 20 to 190 seconds, with the majority in the range of 30 to 50 seconds, have been found (Lippa, 1978).

The multispiked X-ray bursts may be considered as a superposition of several single-spiked events representing the basic units of energy release in flares (Crannell *et al.*, 1978; de Jager and de Jonge, 1978). However, characteristics of these basic units, such as rise and decay times, are not well known because of the limited time resolution of presently available observations.

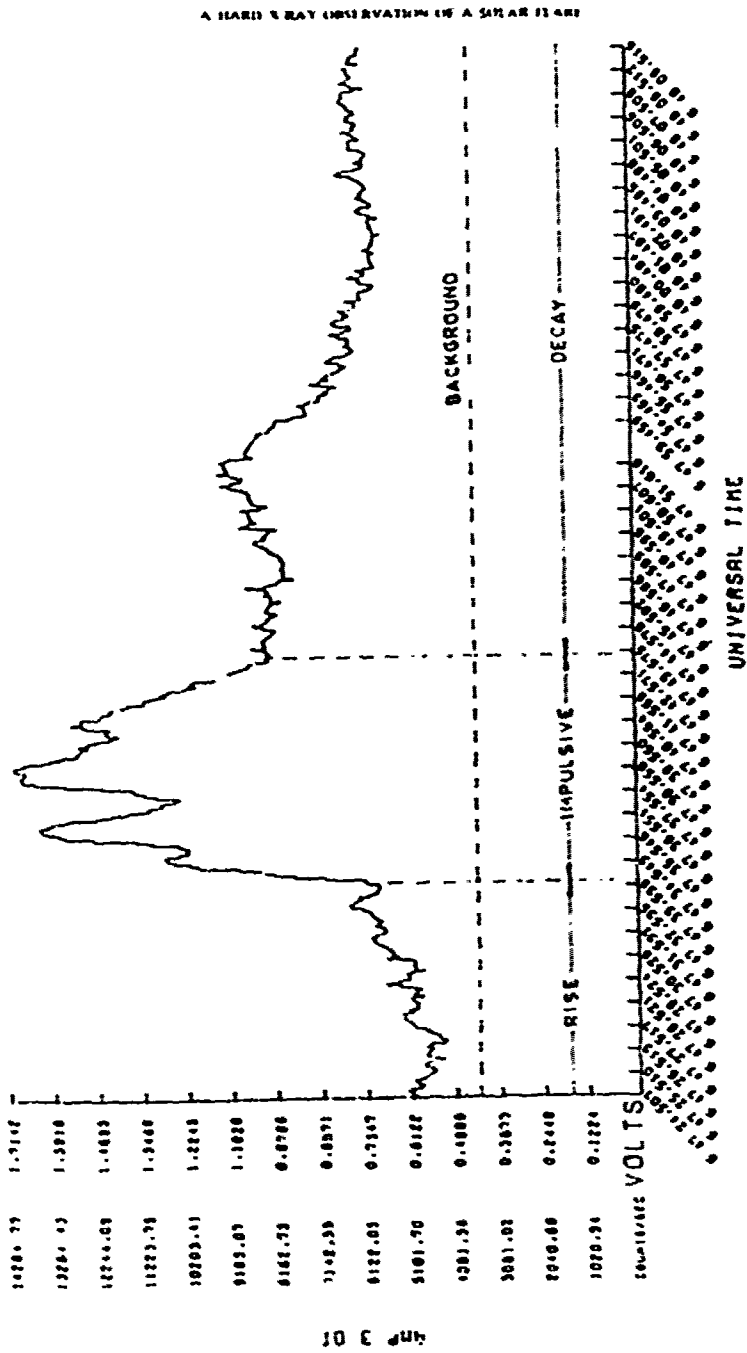


Fig. 5.4 An example of rapid time variations during an impulsive hard X-ray burst observed with a balloon-borne detector having 0.1 s time resolution. The impulsive emission, which lasted for about 0.5 s, consisted of 4 spikes, the e-folding rise time of the first spike being about 1.5 s and the e-folding decay time of the last spike being about 5.8 s (Fluett and Duprat, 1977).

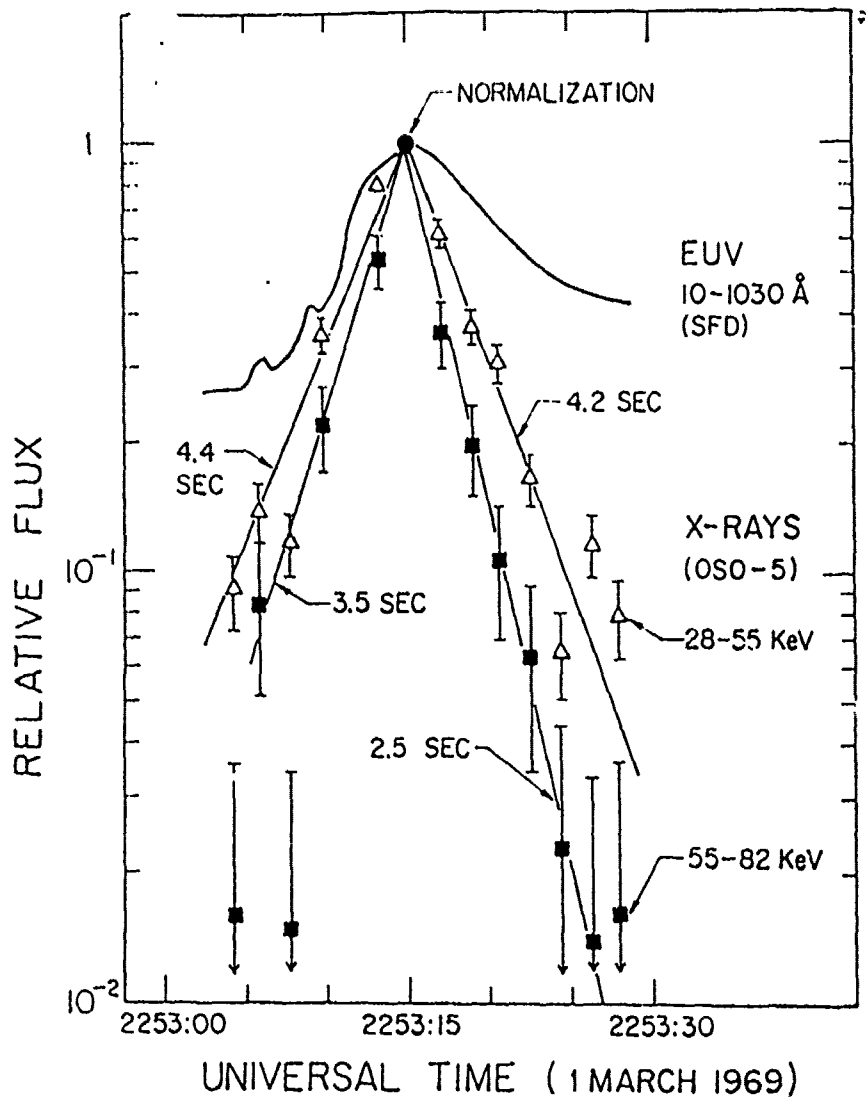


Fig. 5.5 The temporal evolution of the X-ray spectrum during an impulsive hard X-ray burst. The X-ray spectrum hardens with increasing X-ray flux and softens with decreasing X-ray flux, the spectrum being hardest at the X-ray maximum. The rise and decay times for the EUV emission are larger than the corresponding times for X-rays > 28 keV (Kane et al., 1978).

Physical interpretation of the hard X-ray emission requires a determination not only of the time scales of intensity variations, but also of the spectral evolution during a burst. An example of such a spectral evolution is shown in Fig. 5.5. Kane and Anderson (1970) found a characteristic soft-hard-soft evolution to characterize their events, mostly short-duration emission spikes accompanying small flares. These events had fast-rise, slow-decay profiles. Lean (1978) found similar patterns with 10-s time resolution. Occasionally, a time dispersion, with harder X-rays peaking later, has been reported (Bai and Ramaty, 1979). Hoynig *et al.* (1976) found no clearly identifiable trend in some of the flares they observed. However, they and Benz (1977) did find that the soft-hard-soft pattern holds for each spike burst of the multispiked flares of 4 and 7 August 1972. Cannell *et al.* (1978), in a series of mostly shorter-duration events with simple time profiles, found a rise-decay time symmetry with a soft-hard-soft pattern. Thus, a soft-hard-soft evolution of the hard X-ray spectrum seems to be a characteristic feature of the impulsive phase.

5.3.3. Classes of X-Ray Flares

The time variations and spectra of X-ray bursts during the impulsive phase do not permit organization into subclasses. However, the presence or absence of the impulsive phase itself can be used to classify flares. For example, the hard/soft ratio of peak fluxes at 20 keV and 5 keV may be used to characterize the "magnitude" of the impulsive phase of a given flare. We can conceive of gradual flares with virtually no impulsive phase. Although the OSO-7 observations do not seem to show a distinct subclass of thermal only events on the basis of the hard/soft ratio (Datlowe *et al.*, 1979), other observations (Kane, 1969, 1974a; Kane and Anderson, 1978) do indicate the existence of gradual flares with essentially no detectable impulsive phase.

5.3.4. Polarization and Directivity

The principal polarization measurements of ~ 15 keV X-rays have been carried out by the Intercosmos series of satellites and the OSO-7 satellite. OSO-7 observations (Nakada *et al.*, 1974) were examined for a number of events, primarily during August 1972. Because of intercalibration problems between detectors, their results are not certain, but the most probable value for the polarization is less than about 10%. Intercosmos 7 observed polarization of the same order in the flare of 4 August 1972 (Lindo *et al.*, 1973). More recent observations by SOLRAD (Doschek, private communication) and Intercosmos 11 (Lindo *et al.*, 1976), which were rotating devices to remove intercalibration problems, were hampered by a lack of intense X-ray events during solar minimum. The Intercosmos 11 experiment saw not more than a few percent polarization in a 6 July 1974 event, but this observation may not have covered the impulsive phase.

Directivity in the hard X-ray emission has been sought on a statistical basis by looking for center-to-limb variations in the peak X-ray flux or spectral hardness of different X-ray bursts. On the assumption of a constant geometry from flare to flare, one can count the rate at which events larger than a certain threshold occur as a function of location on the sun. Ohki (1969), Pinter (1969), and Phillips (1973) independently studied a set of X-ray bursts from OGO-1 and OGO-3 (Arnoldy *et al.*, 1968). They found, respectively, a maximum in the center of the

disk, a maximum at $\pm 50^\circ$ longitude, and no center-to-limb variation at all in the frequency of burst occurrence, inconclusive and conflicting results.

More definitive center-to-limb hard X-ray studies have been carried out by Kane (1974b) and Datlowe *et al.* (1977). Datlowe *et al.* used hypothesis-testing techniques to check the significance of their results and used the soft X-ray burst location to reduce the model-dependence. No center-to-limb variation was found in either study. Datlowe *et al.* (1977) have claimed an upper limit of 40% for the total variation at 95% confidence level and inferred that this ruled out strong streaming motions of the X-ray emitting electrons.

Since hard X-ray directivity is energy dependent, it could cause center-to-limb variations in the spectra of hard X-ray bursts. Roy and Datlowe (1975) reported that spectra were characteristically steeper (softer) at the limb. To produce this variation would require very large center-to-limb intensity variations, well beyond the upper limit found by Datlowe *et al.* (1977).

It is important to note that the claims regarding absence or presence of directivity of the hard X-ray emission are dependent on the assumptions regarding the model of the hard X-ray source and adequate corrections for the low sensitivity in identification of flares near the limb. Corrections for X-ray albedo (Henoux, 1975) may also be important. The present status of the searches for polarization and directivity in hard X-ray bursts is a collection of null or inconclusive results. More sophisticated tests are required to observe these phenomena properly.

5.4 RADIO EMISSION

The main components of radio emission during the impulsive phase are the Type III bursts at meter-decimeter wavelengths and impulsive continuum radiation, occasionally with superposed fine structure at centimeter-decimeter wavelengths (cf. Kundu, 1965). The Type III bursts are characterized by their brief duration of 1 or 2 seconds around 100 MHz and a rapid drift at a rate of about 100 MHz per s from high to low frequencies. The special significance of Type III bursts in relation to solar flares is their occurrence in compact groups of intense bursts marking the impulsive phase (cf. Kane, 1972a; Stewart, 1978). An example is shown in Fig. 5.6. The Type III bursts are generally interpreted as due to plasma radiation from 10-100 keV electrons suddenly ejected in repeated bursts of less than about 1 s duration. The Type III electrons travel along open field lines (Wild, 1964), with typical velocities of about $c/3$, out through the corona into the interplanetary medium, as confirmed by in situ observations (Lin, 1973). Frequently Type V and Occasionally Type "U" bursts have also been observed in association with simple impulsive microwave events (Crannell *et al.*, 1978), although the time coincidences were not as good as in the case of simple Type III bursts. The observation of such "U" bursts implies that in these flares magnetic field lines at coronal levels above the active region were closed.

A typical microwave impulsive burst is characterized by a rapid rise (less than about 30 s) to maximum and a slightly slower decay (< 1 minute), followed by a post-burst tail with a few minutes duration. The radiation is continuum in nature and is believed to be due to gyrosynchrotron radiation of intermediate energy electrons (~ 100 -500 keV) spiralling in the sunspot-associated magnetic field of several hundred gauss. The radiation is polarized, 10-40%, generally in the extraordinary mode at higher frequencies (10-4 GHz) and in the ordinary mode at

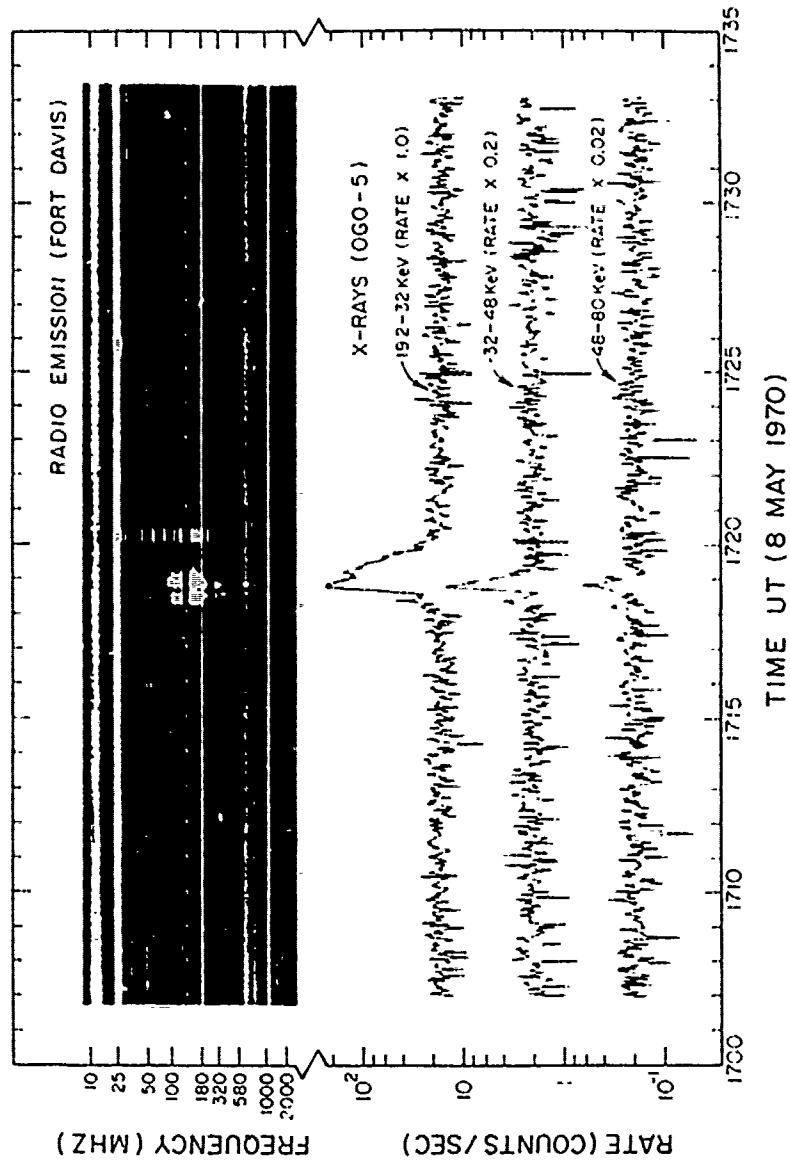


Fig. 5.6 An example of the occurrence of a Type III radio burst during the impulsive phase of a flare. Note the similarities between the temporal structure of the radio and X-ray emissions (Kane, 1975).

lower frequencies (< 2 GHz) (Tanaka and Kakinuma, 1962). The reversal in the sense of polarization arises, according to Takakura (1960), from the fact that there is a sharp decrease in the extraordinary flux density at the gyrofrequency ω_{UH} of thermal electrons, while lower frequencies ($< \omega_{UH}$) in the ordinary mode still escape.

The flux-density spectra of two microwave bursts are shown in Fig. 5.7. The spectra of most centimeter bursts at the peak of the impulsive phase shows a sharp rise in intensity from < 1 GHz to about 5 GHz and then decrease more or less steeply toward short centimeter and millimeter wavelengths (cf. Guidice and Castelli, 1973). Sometimes, the spectrum exhibits a "thermal-like" behavior in the sense that the burst intensity increases with increasing frequency until about 2 GHz, followed by a region in which the intensity is independent of frequency. However, the number of impulsive bursts having this kind of spectrum is very small. Both kinds of spectra have been interpreted as due to synchrotron self-absorption and/or thermal gyroresonance absorption (see, e.g., Takakura, 1972; Ramaty and Petrosian, 1972).

There have been abundant observations of impulsive radio bursts at fixed frequencies, but without spatial resolution. Extensive interferometric observations with intermediate (\sim arcmin) spatial resolution have been made at Toyokawa (cf. Enome and Tanaka, 1973), but high spatial resolution has been achieved only recently and for limited periods. Early observations by Kundu (1959) showed that the centimeter burst source starts with a size of slightly smaller than $1'$ arc, condenses into a smaller region ($\lesssim 1'$ arc) during the impulsive phase, and then expands to a size of $3'$ arc during the post-maximum decay phase. The burst is polarized mainly during the impulsive phase, the post-burst phase being essentially unpolarized. Recent, high-resolution interferometric observations by Hobbs *et al.* (1973) and Kundu *et al.* (1974) have provided valuable information on the existence of fine structure in the burst sources. One-dimensional fan-beam observations with a resolution of $6''$ arc at 6 cm by Alissandrakis and Kundu (1978) have confirmed the polarization and spatial characteristics of microwave bursts on a scale of several arc seconds and have revealed several other interesting features. Bursts of intensity 1 to 10 sfu (10^{-22} Wm $^{-2}$ Hz $^{-1}$) occur quite often near the neutral line of the magnetic field, as determined by the polarization maps of 6-cm active regions (Kundu *et al.*, 1977). At the time of maximum, the brightness temperatures can reach 10^8 K and the angular size is generally about $10''$ arc, or less. After the maximum, the burst core expands up to a size of $>$ about $1'$ arc, and the brightness temperature is generally near 10^6 K. At 3.7 cm, the burst source often starts with a precursor of $4''$ arc, condenses to a minimum size of $2''$ arc at the peak of the burst, after which the source expands to a size of $5''$ arc, or larger. In a complex burst with several maxima, the burst sources are located at different positions; this positional change is similar to the behavior of H α flares, which often have more than one maximum, each maximum corresponding to a small-diameter "kernel" (Enome and Tanaka, 1973; Alissandrakis and Kundu, 1975).

Only one sense of circular polarization over the entire extent of the burst sources (Fig. 5.8) was observed by Alissandrakis and Kundu, 1978. This suggests that if the burst was associated with loop structures, the emission must have been associated with one leg of the loop. The fact that no polarization is observed in the post-burst phase implies that the energetic electrons responsible for gyro-synchrotron radiation during the impulsive phase must be thermalized in the

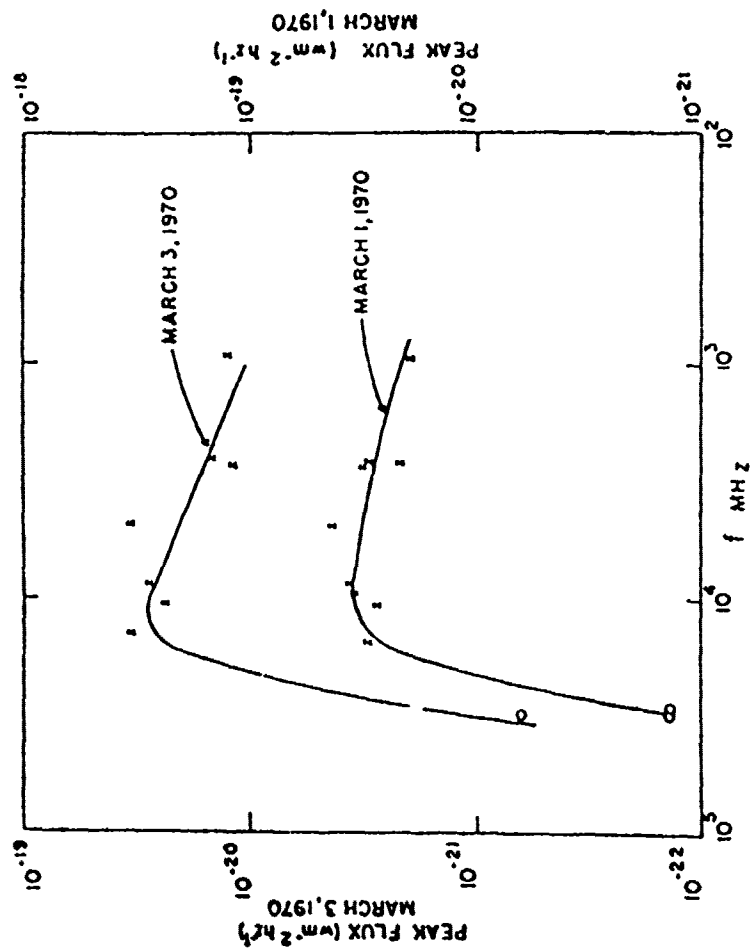


Fig. 5.7 The flux-density spectra of the bursts observed on 1 and 3 March 1970. The values at wavelengths other than 9 mm were taken from Solar Geophysical Data (Kundu and Liu, 1973).

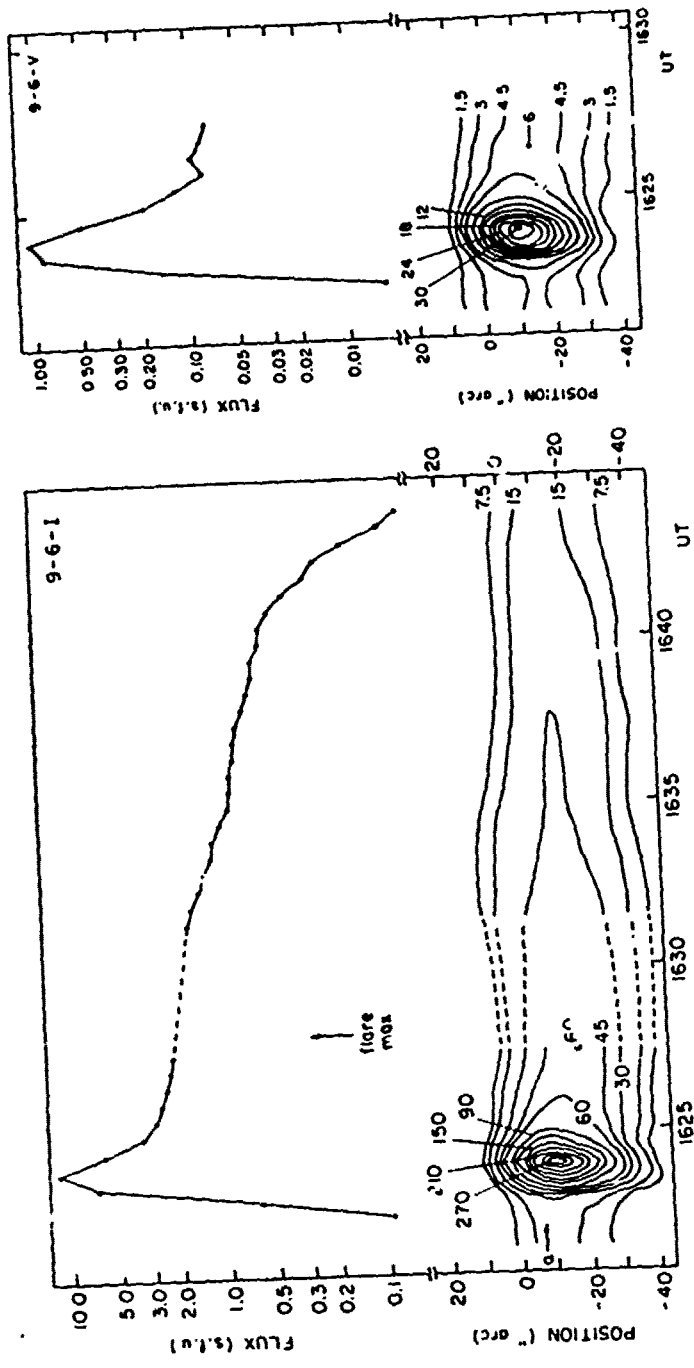


Fig. 5.8 Total density (I) and circular polarization (V) data of a burst observed on 8 May 1974 with the Westerbork Synthesis Radio Telescope at 6 cm with 6" arc resolution. The upper part of the figure shows the flux in solar flux units ($1 \text{ sfu} = 10^{-22} \text{ Wm}^{-2} \text{ Hz}^{-1}$) as a function of time, while the lower part shows the brightness temperature as a function of one-dimensional position and time. Contour labels are in units of $10^6 \times \text{arcsec}$. Positive polarization values (solid contour line) correspond to right-hand circular polarization. Dashed contours indicate a gap in the observations. The arrow on the I contour map shows the position of a constant source that has been subtracted.

post-burst phase. The thermalization of the nonthermal electrons alone cannot explain the emission in the post-burst phase; there must exist at the same time a larger number of lower energy electrons (cf. Neupert, 1968; Hudson and Ochi, 1972), which will contribute to the post-burst phase emission. The unipolar nature of the microwave source could be interpreted as evidence of the existence of asymmetrical bipolar magnetic fields in which the accelerated electrons are located (Kundu and Vlahos, 1978). Specifically, the observations suggest that over the stronger pole (of field strength near 600 gauss) the electrons have large pitch angles and therefore they radiate efficiently at 6 cm, whereas over the weaker pole (field strength 100–200 gauss) the electrons have smaller pitch angles, so that they either penetrate toward the chromosphere where they produce X-rays, or radiate efficiently only at longer wavelengths (about 20–30 cm) because of weaker field and smaller pitch angles. In the cases where the magnetic field in the two polarities is similar or when the burst is very strong, one should observe both sense of polarization at one particular wavelength, in agreement with the observations of Enome *et al.* (1969).

5.5 EUV, XUV, AND SOFT X-RAY EMISSION

An example of an impulsive EUV burst was shown in Fig. 5.1. The impulsive phase, as defined by the hard X-ray and microwave bursts, is marked by similar events in the XUV and EUV radiation emitted over the temperature range of 10^4 to 10^6 K. However, unlike the hard X-ray and microwave wavelength regions, the 10–1000 Å region contains both line- and continuum-emission components during solar flares. Measurements of line emission provide a potentially powerful diagnostic tool for determining characteristics such as temperature, emission measure, and density of the radiating region. When interpreting line emission over the EUV/XUV/soft X-ray spectrum, it is important to appreciate that correlation of high temperature with shorter wavelength is only approximate. There are several notable exceptions (e.g., both OVII 21.6 Å and Mg X 625 Å are emitted at about 1.5×10^6 K). We shall therefore try to refer to the emitting temperature when reviewing observations, rather than designate only the wavelength band.

Line spectra relating to the impulsive phase have now been observed with a number of instruments. Some of the earliest data were recorded by the AFCRL instrument on OSO-3, which operated in the range of 270 to 1310 Å (Hall and Hienteregger, 1969; Hall, 1971). These included, in particular, a number of chromospheric and coronal lines covering the range 10^4 to 2.5×10^6 K. The data had good time resolution (about 0.16 s), but were spatially integrated over the entire disk.

The Harvard experiments on OSO-3 and OSO-5 made some useful measurements, (Wood *et al.*, 1972; Donnelly *et al.*, 1973), but it is with OSO-7 and Skylab that most of the recent data has been obtained. On OSO-7, the Goddard instrument package consisted of two filtered telescopes covering 120–400 Å (Neupert *et al.*, 1974). These instruments had a spatial resolution of 5 arcsec. On Skylab, flares were recorded by the NRL spectroheliograph and slit spectrometer, as well as the Harvard polychromator. In most of these measurements, the impulsive phase of the flare was missed because of relatively poor time resolution. Even the observations of "impulsive" solar EUV bursts recently reported by Emslie and Noyes (1978) probably relate to small-scale, secondary brightenings rather than to flares themselves.

The Lebedev Institute experiment (Grineva et al., 1973) flown on the satellite Intercosmos 4 has recorded the finest spectrum of the important iron lines at 1.9 Å. Unfortunately, the limited operational flexibility of the satellite led to a very small amount of data, so that good records are not available during the impulsive phase.

Information on spatial distribution of the EUV has been obtained from the OSO-7 data (Neupert et al., 1974). During the impulsive phase, the EUV follows the neutral line closely, and is somewhat similar to the H α flare. Hotter material corresponding to Fe XXV 1.9 Å appears to come from arches overlying this structure. In a slow-rising flare, Rust et al. (1975) have observed impulsive EUV emission confined to the center of an activated filament. The emission increased again some eight minutes later when the filament disrupted. It has been suggested that this observation supports the concept of the flare trigger arising from interaction between newly emerging flux and the twisted-filament flux.

The major increase in the EUV emission seems to originate in the upper chromosphere and transition region (Hall, 1971). The density-dependent lines indicate an enhancement in density during the impulsive phase (Hall, 1971; Noyes, 1973). Compared to the chromospheric and transition-region lines, H α seems to have a slower rise and a later peak, while coronal lines show a much slower rise, with virtually no impulsive component. This is broadly consistent with the results from OSO-7 (Neupert et al., 1974), but Neupert finds that the impulsive phase is evident up to temperatures of 2.3×10^6 K (Fe XIV). While this is the general picture, there are also cases from OSO-3 (Neupert, unpublished) where the soft X-ray maximum precedes the XUV maximum. In evaluating this apparent discrepancy, however, it should be remembered that OSO-3 data comes from integrated disk radiation, and could be misleading.

A major difficulty with the line measurements in the past has been their poor time resolution. This was particularly true for instruments with fine spatial resolution because of difficulties in recording the large matrix of space and time points. The conclusions drawn from these observations with regard to the impulsive phase should therefore be considered only suggestive. Significant improvement is expected from the forthcoming Solar Maximum Mission, which is specifically designed for observing flares.

A ground-based technique, exploited by Donnelly (1968, 1973), relies on the absorption of the EUV radiation by the Earth's ionosphere to produce sudden frequency deviations (SFD). It is possible to reproduce the time-history of the total emitted radiation in the 10 to 1030 Å range, although such a technique tends to favor stronger lines (e.g., He I 584 and He 301). Although the measurements do not have any spatial resolution, they do provide continuous daytime coverage of the sun with a high temporal resolution (~ 1 s). Consequently, several hundred EUV bursts have been recorded. The observed Central Meridian Dependence (CMD) of the occurrence frequency of these bursts, shown in Fig. 5.9 indicates that the impulsive EUV emission originates in more than one small source ("kernels") in the flare region, some of these sources being shallow and others deeply embedded in the chromosphere, as shown, for example, in Fig. 5.10b. The nonflaring solar atmosphere outside the source, assumed to be like the upper chromosphere (10^4 – 10^5 K), causes occultation of individual EUV sources when viewed from large angles and thus gives rise to the observed CMD dependence.

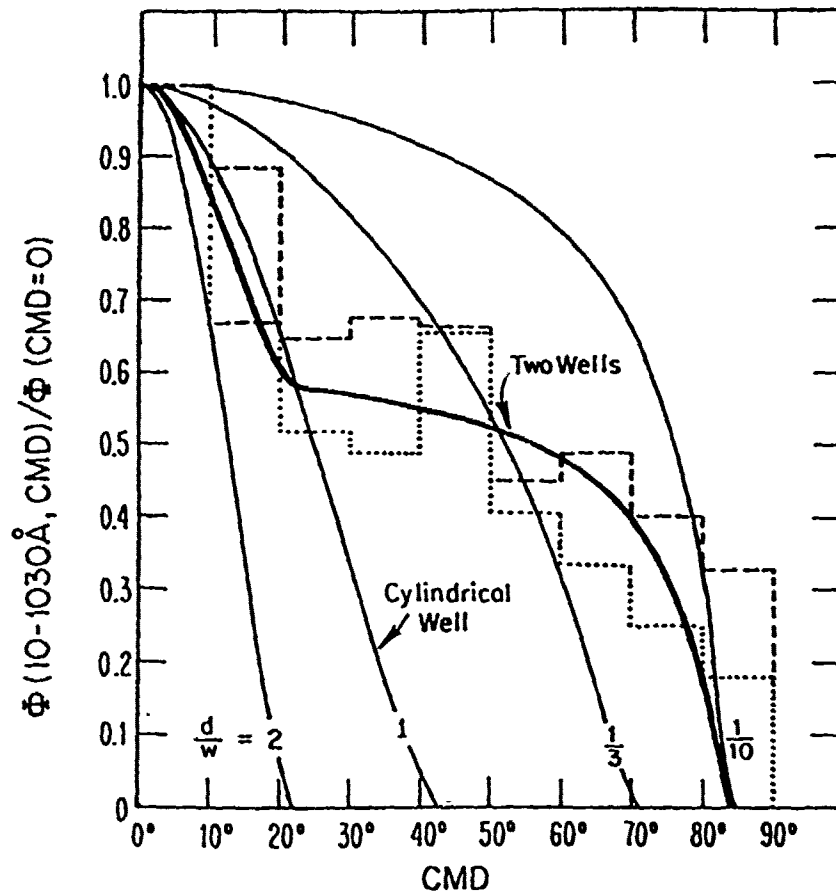
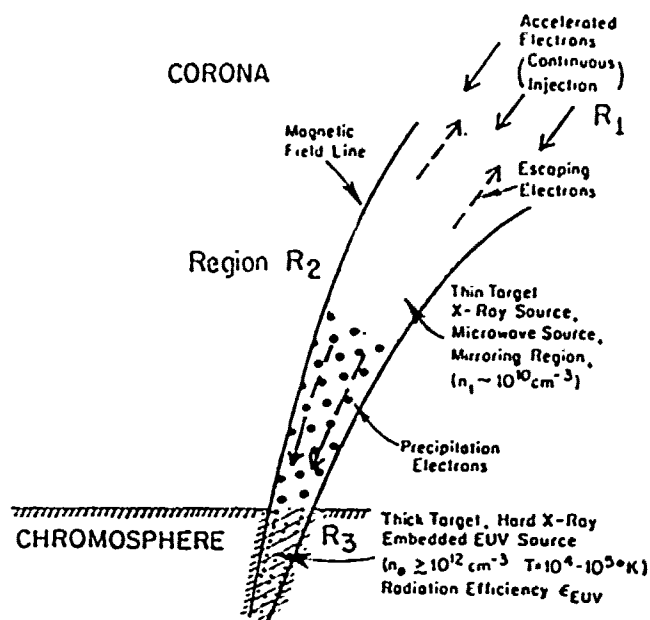
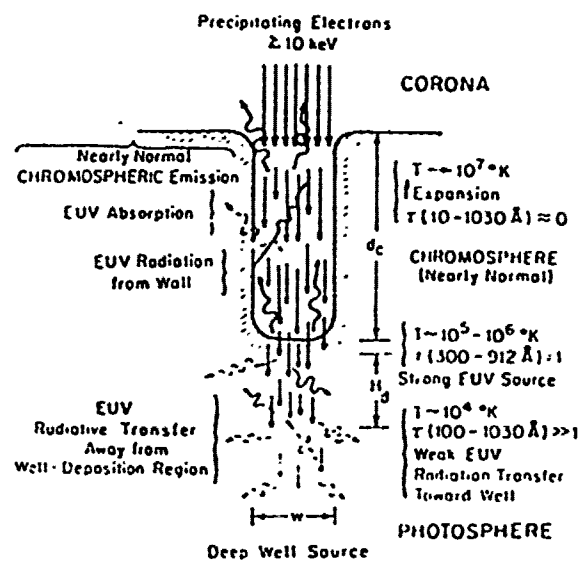


Fig. 5.9 Comparisons of the observed (histograms) Central Meridian Distance (CMD) dependence of impulsive LUV bursts observed via SFDs and the expected CMD dependence (solid curves) for embedded cylindrical-well EUV sources with different depth (d) to width (w) ratios. Each LUV source is assumed to be optically thin, and the emission from the sides of the cylindrical well is assumed to be negligible compared to the emission from the bottom surface. Occultation of a part of the source area by the surrounding chromosphere gives rise to the CMD dependence. A satisfactory explanation of the observations requires the presence of two or more small LUV sources ("kernels") in most impulsive flares (Donnelly and Kane, 1978).



(a) Precipitation Model



(b) Low-Efficiency EUV Source

Fig. 5.10 Schematic model of impulsive hard X-ray and EUV sources. If the precipitation efficiency is high ($\epsilon_p \approx 1$), then the thick-target region dominates the hard X-ray burst for disk flares, and the EUV radiation efficiency ϵ_{EUV} must be low. If the thin-target emission dominates, then $\epsilon_p \ll 1$ and ϵ_{EUV} may be high, ~ 1 (Donnelly and Kane, 1978).

5.6 OPTICAL EMISSION

The optical components of the impulsive phase appear to be spatially limited to certain small points, or kernels, within the flare. A number of authors within the last decade have drawn attention to these kernels, usually observed in H α , which correspond approximately in time with spikes in hard X-rays and microwaves (de Jager, 1967; Vorpahl and Zirin, 1970; Zirin *et al.*, 1971; Vorpahl, 1972, 1973; Zirin, 1978). It is important to distinguish between the kernel emissions and those emissions associated with the extended (total area) H α flare; the latter show a closer temporal relation with the thermal aspects of the flare (e.g., Švestka, 1976). Apart from their close temporal relation with other impulsive emissions, the kernels, according to Vorpahl (1972), are also characterized by the broad line profile of H α emission.

The light curves for the kernels observed by Vorpahl lagged the associated hard X-ray profiles by about 20–30 s in their onset and peak. This lag, however, was not found in the observations by Zirin (1978); instead, the light curves in H α were found to match the X-ray profiles to within the experimental resolution (± 3 s) during their onset and rise to intensity maximum. Thus, the temporal relationship between H α and other impulsive emissions is not completely clear at the present time.

Vorpahl's (1972) observations indicated that when pairs or multiple kernels occurred, their locations were near the magnetic inversion line and in regions of opposite magnetic polarity. Furthermore, these regions were apparently connected by common field lines, as judged by fibril configurations. Zirin and Tanaka (1973) observed a number of short-lived (5–10 s) bright points with the $\lambda 3835 \text{ \AA}$ filter (15 \AA band) during the flare of 2 August 1972. The filter's bandpass contained the H β line, therefore it is not clear whether these points were continuum emission or H β line emission (Švestka, 1976). These points occurred in pairs lying on opposite sides of the inversion line and their appearance corresponded in time with individual peaks in the associated hard X-ray burst.

It is important to note that in these observations, an X-ray peak, when associated with an optical counterpart, had a tendency to be keyed to the brightening of a particular point, or pair of points, and not to a repeated brightening of the same point, or pair of points. This suggests that the impulsive phenomenon may consist of an energy release which occurs only once at a given location within the flare. A similar effect is indicated in H α (Zirin, 1978) and in the EUV observations (Thomas and Neupert, 1975). Furthermore, the spatially-resolved microwave observations made by Enome and Tanaka (1973) showed that for several flares the individual components of the microwave burst occupied different sites within the active region. Thus, even the microwave observations are consistent with the single occurrence of impulsive emission at a given location in the flare.

In addition to revealing a temporal relation between H α and hard X-ray emission, Zirin's (1978) observations have shown that the impulsive growths of H α emissions in various distant sections of individual flares occur within seconds of each other. These nearly simultaneous brightenings are indicative of a rapidly propagating disturbance with speeds greater than 5000 km s^{-1} .

White-light observations (what few there are) have shown that the appearance of the continuum emission knots in energetic flares corresponds in time to the

impulsive phase (see review by Švestka, 1976). In the well-known flare of 7 August 1972, Rust and Hegwer (1975) observed the white-light intensity curve to follow the hard X-ray profile in considerable detail. The continuous emission in white-light flares is located within the brightest H α strands located on each side of the magnetic inversion line (cf. De Mastus and Stover, 1967; Slonim and Korobova, 1975); this observation suggests the coherent picture that the white-light flare emission, like the H α kernels, is a phenomenon occurring at the footpoints of the magnetic arches that span the inversion line.

Sufficient spectral data are not presently available to determine the origin of the optical continuum in flares (see review by Švestka, 1976). It has been suggested that the emission is the response to bombardment of the photosphere by high-energy protons (cf. Švestka, 1970; Najita and Orall, 1970), or of the chromosphere by electrons resulting in enhanced recombination continuum (cf. Hudson, 1973; Lin and Hudson, 1976). In either case, the white-light continuum seems to have a direct relationship to the high-energy particle characteristics of the flare. If the white-light emission is indeed an impulsive-phase phenomenon occurring prior to the second-stage acceleration, then energetic electrons are probably the primary source of energy for the white-light emission.

An interesting spectral effect regarding the two principal kernels in flares (lying on opposite sides of the inversion line) is that the kernel located in the region of weaker magnetic field strength seems to have the larger H α line width (Neidig, 1976). This is consistent with a flare model consisting of an asymmetrical, bipolar, field configuration in which electrons preferentially precipitate to chromospheric levels at the pole with weaker field strength; such a model is also consistent with the high-resolution microwave observations described in Section 5.4.

Model calculations have shown that large fluxes of high-energy electrons penetrating the chromosphere should result in large H α line widths (Canfield, 1974; Brown et al., 1978). Observations of the development and decay of the H α line width during a flare might, therefore, provide information on the characteristics of penetrating electrons during the optical impulsive phase. The available observations, which typically have a time resolution of about 1 minute, follow the gross features of the associated microwave bursts (cf. Janssens and White, 1970). Also, the peak H α line width in a flare seems to be related to the peak fluxes in the associated hard X-ray and microwave bursts (Neidig, 1978). The occurrence of white-light emission in flares has been known to be associated with large H α line widths (Slonim and Korobova, 1975; Neidig, 1978). However, quantitative observations with higher (about 1 s) time resolution are essential for determining precisely how the H α emission from the kernels is related to the development of the impulsive phase.

5.7 RELATIONSHIPS AMONG X-RAY, EUV, OPTICAL, AND RADIO EMISSIONS

The characteristics of X-ray, EUV, optical, and radio emissions observed in solar flares depend on different aspects of the flare environment. Taken together, they provide complementary evidence of the role of energetic electrons in the flare process. Average quantitative relationships among impulsive hard X-ray, EUV,

and microwave fluxes have been deduced from observations of a large number of flares (Kane, 1973; Donnelly and Kane, 1978; Hudson *et al.*, 1978). Similar quantitative information about the optical fluxes is not yet available. We will therefore confine our discussion primarily to the role of energetic electrons in exciting the hard X-ray, EUV, and microwave emissions. With regard to the optical emission, we only mention here that it, too, could be excited indirectly by energetic electrons, as has been suggested, for example, by Zirin *et al.* (1971), Hudson (1972), Brown *et al.* (1978), and Zirin (1978).

While the hard X-ray and microwave emission is related to the population of energetic electrons inside the flare region, the Type III radio emission is related to the 10–100 keV electrons escaping into the corona. The hard X-ray, microwave relationship yields the relationship between the X-ray emitting electrons and the electrons located in the microwave source, where the magnetic field is expected to be several hundred gauss and the ion density is $<$ about 10^{10} cm^{-3} . Since it is the higher energy part of the electron spectrum that contributes more to the microwave emission, the deduced parameters are characteristic of electrons with energy $>$ about 100 keV.

On the other hand, the hard X-ray, EUV relationship relates the X-ray emitting electrons to the energy deposited in the EUV source, which is expected to be a relatively low-temperature region with the hydrogen density $\geq 10^{12}$ cm^{-3} (Kane and Donnelly, 1971; Hudson, 1972). Thus, if the energy is transported primarily by energetic electrons, the deduced parameters are characteristic of electrons with energy ~ 10 keV.

5.7.1. X-Ray, Radio Relationship

Since the early reports by Peterson and Winckler (1959) and Kundu (1961), simultaneous hard X-ray and microwave observations of impulsive solar flares have shown that these emissions are generally well correlated in time and occur in coincidence with other impulsive (flash-phase) emissions (Arnoldy *et al.*, 1968; Kane, 1972b, 1973). The microwave energy flux S_r has been found to be approximately proportional to the energy flux S_x in high-energy ($>$ about 20 keV) X-rays observed at the maxima of a large number of X-ray bursts. $S_x/S_r \sim 10^7$, where the units for S_x and S_r are $\text{erg cm}^{-2} \text{s}^{-1}$ and $10^{-22} \text{Wm}^{-2} \text{Hz}^{-1}$ respectively. No direct relationships have been found between the X-ray and microwave spectral distributions, except for individual events such as the August 1972 flares studied by Benz (1977). As for other observational characteristics, the data of X-ray polarization and spatial distributions are too sparse to support any general conclusions in relation to radio spectra.

In a study of a special class of burst made by Crannell *et al.*, (1978), hard X-ray bursts with a relatively simple time structure were selected from the observations obtained with the OSO-5 X-ray spectrometer. These data confirm the time-intensity correlations reported by Kane (1973, 1974a) and exhibit a symmetric structure in the rise and fall of the X-ray emission. U-bursts preceded most of the simple X-ray spike bursts for which meterwave radiation was reported. Type V and Type II bursts were also common in these events. A variable delay of the microwave peak with respect to the X-ray peak emission and a longer microwave fall time compared to the X-ray fall time were found in these events. The most probable value of the delay for 10 GHz was 2 seconds, as seen, for example, in

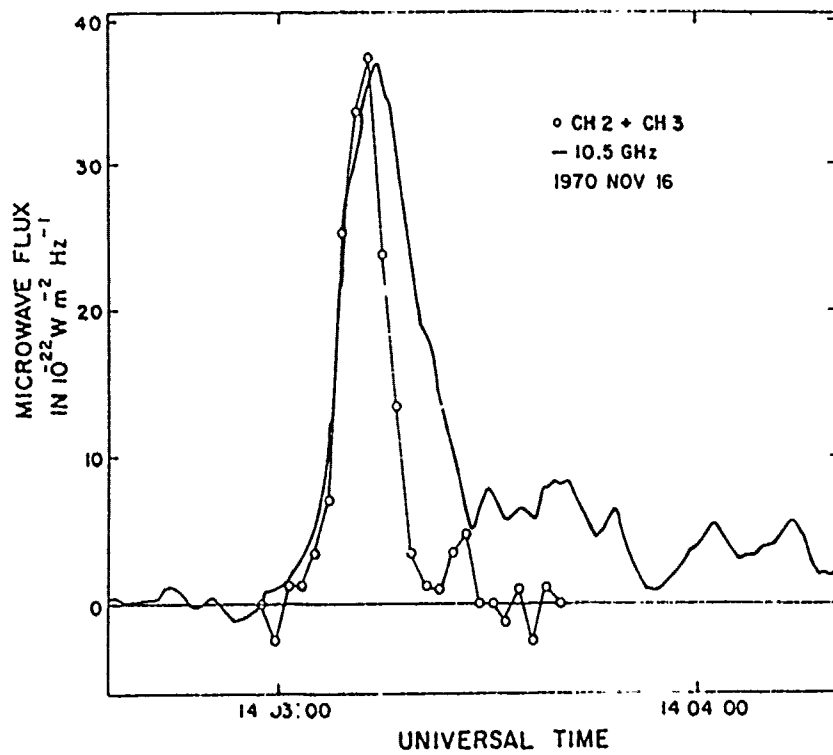


Fig. 5.11 An example of the delay between the maxima of impulsive hard X-ray and microwave emission (Crammel et al., 1978).

Figure 5.11. The peak microwave emission was found to be most strongly correlated with the time integral of the X-ray emission.

About 30% of microwave and hard X-ray impulsive bursts are associated with Type III bursts (Kane, 1972a; McKenzie, 1972). Moreover, the correlation between the impulsive hard X-ray and the Type III bursts tends to increase systematically with the increase in the hardness of the X-ray spectrum (Kane, 1975). These observations are consistent with the suggestion by de Jager and Kundu (1963) that only part of the accelerated electrons escape into the corona and generate Type III bursts, while other electrons move downward to lower levels to produce microwave and hard X-ray emission.

Detailed characteristics of the magnetic field topology and the acceleration process probably determine the relationship between these two electron populations. Further understanding of the related processes requires measurements with high spatial resolution at both microwave and hard X-ray wavelengths. However, while positional measurements of microwave-burst sources with spatial resolution of a few arc seconds are now being made (cf. Alissandrakis and Kundu, 1978), such data for hard X-ray bursts are not yet available. For three flares studied by Kundu *et al.* (1976), a comparison of the high-resolution microwave data and the simultaneous Skylab soft X-ray data obtained with similar spatial resolution shows that at the impulsive phase the soft X-ray flare kernels are co-spatial with a part of the microwave-burst source, and that the two co-spatial sources have angular sizes of about 5" arc. Alternatively, other studies of the Skylab data involving a much larger number of events indicate that there is no direct correlation between soft X-ray kernels and impulsive phases of flares (Voipahl *et al.*, 1975; Kahler *et al.*, 1976).

We now consider some questions related to the interpretation of the hard X-ray, microwave relationship. It is generally accepted that the emission mechanisms for the impulsive hard X-ray and microwave emissions are respectively the bremsstrahlung and gyrosynchrotron radiation from energetic ($>$ about 10 keV) electrons (cf. Koichak, 1971). The principal questions to be resolved are: (1) Is a single electron population responsible for both the X-ray and microwave emissions? (2) What is the nature of the electron distribution inside the radiation source(s)—thermal (Maxwellian) or nonthermal (non-Maxwellian, e.g., power law)?

Assuming that the X-ray and microwave emissions are emitted by the same electron population, Peterson and Winckler (1959) calculated a magnetic field strength of about 1000 gauss for the source region. However, comparison of the X-ray and microwave intensities led to the conclusion that only 0.01% of the microwave radiation escaped from the source. An alternative explanation was that the microwave-emitting electrons were near 10^9 times fewer in number than those emitting the X-rays. A possible resolution of this apparent "discrepancy" has been widely discussed in the literature (cf. Takakura, 1973). Peterson and Winckler noted that the microwave radiation field is tightly coupled to the emitting electrons. This speculation was confirmed by Ramaty (1969) with calculations of self-absorption and the Razin effect applied to solar flares. Holt and Ramaty (1969) reviewed earlier attempts to interpret the observed temporal and spectral characteristics of associated X-ray and microwave bursts, including the work of Kundu (1961), Anderson and Winckler (1962), Takakura and Kai (1966), and Cline *et al.* (1968). With detailed calculations of electron bremsstrahlung and

gyrosynchrotron emission and absorption, Holt and Ramaty showed that the observations of the large event in July 1966 are consistent with a single source of electrons with energies from 100 to 500 keV.

The thermal versus nonthermal interpretation of the electron distribution has been discussed extensively in the literature (cf. Arnoldy *et al.*, 1968; Kahler, 1975). An unambiguous answer is not yet available. The dependence of the hard X-ray spectrum on the electron spectrum is relatively simple, but the existing data cannot distinguish between a thermal and a nonthermal electron distribution. In addition to the problems relating to deducing the electron spectrum from the hard X-ray spectrum observed with the presently available spectral resolution (cf. Brown, 1978; Liu, 1979), the detailed characteristics of the hard X-ray source and contribution from X-ray albedo (Tomblin, 1972; Henoux, 1975; Langer and Petrosian, 1977; Bai, 1977) may substantially affect the interpretation of the X-ray observations.

The interpretation of the microwave observations is ambiguous because of the competition between various emission and absorption mechanisms (cf. Ramaty and Petrosian, 1972). An additional complication arises from the dependence of gyrosynchrotron emission on the structure of the magnetic field (Takakura, 1973; Mätzler 1976). Thus the conclusions drawn from the microwave spectra are strongly model dependent.

The interpretation of the microwave spectra is simpler in the optically thick portion of the spectrum, especially for Maxwellian distributions of electrons. Assuming this to be the case, using the temperature $10 \lesssim kT \lesssim 60$ keV deduced from hard X-ray observations, Crannell *et al.* (1978) found areas of order 10^{18} cm² for the microwave-emitting region. For homogeneous, isotropic sources common to both X-ray and microwave emission, densities of order 10^9 cm⁻³ were obtained. The validity of these assumptions is presumably supported by the good correlation between the area and the duration of the X-ray bursts.

Mätzler *et al.* (1978) have investigated the implications of the thermal model based on the above analyses. They assume that the heating and cooling of the plasma results, respectively, from the adiabatic compression and expansion. This predicts a simple relationship between the temperature and emission measure: $EM \propto T^{3/2}$, which they find is consistent with their observations of the 1 March 1970 flare event (Fig. 5.12). The OSO-7 observations of similar events, however, do not follow this simple pattern (Lean, 1978); instead, the emission measure in a thermal fit tends to increase throughout the impulsive phase, even when the temperature is decreasing. Clearly, further observations and analysis are needed in order to establish the relationship between the emission measure and temperature.

5.7.2. X-Ray, EUV Relationship

So far, most of the studies of the hard X-ray, EUV relationship have been based on the broad-band (10–1030 Å) EUV measurements made via Sudden Frequency Deviation (SFD) (Kane and Donnelly, 1971; Donnelly and Kane, 1978; Emslie *et al.*, 1978; Kane *et al.*, 1978). The studies by Donnelly and Kane indicate that the maxima of the impulsive hard X-ray and EUV emissions are coincident with ± 1 s. Moreover, the EUV emission is consistent with the production by 10–25 keV electrons, moving down into the upper chromosphere and producing a quasi-thermal plasma.

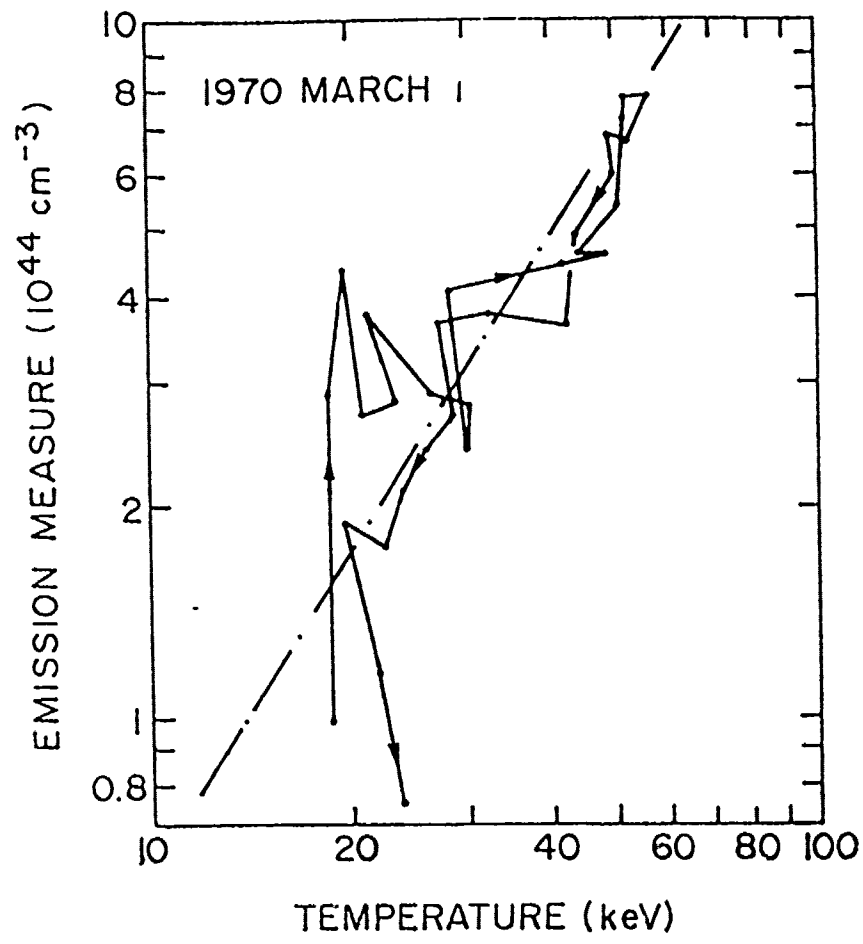


Fig. 5.12 A regression plot (solid line) between the emission measure (EM) and temperature (T) during an impulsive hard X-ray and microwave burst. The dashed line is a computed relationship for an adiabatic thermal model of the sources (Matzler et al., 1978).

A comparison of the total energy of the accelerated electrons, as deduced from hard X-ray emission, and the total EUV radiated energy indicates that there may be only a "partial" precipitation of electrons in the chromosphere, the bulk of electrons being confined to lower-density regions (Lmslie *et al.*, 1978; Donnelly and Kane, 1978) as shown, for example, in Fig. 5.10a. Further, the efficiency of the EUV emission, as determined by the ratio of the energy radiated in EUV to the energy input to the EUV-source region, could be $\ll 1$. A possible source structure, which would give rise to such a low EUV-emission efficiency, is shown in Fig. 5.10b. Donnelly and Kane have suggested a careful search for impulsive radiation in the UV range, where a substantial emission energy is expected.

5.8 MODELS OF THE IMPULSIVE PHASE

5.8.1. Classification of the Models

In this section, we discuss models that describe the impulsive phase in terms of the behavior of energetic particles, particularly electrons, in various magnetic field configurations. We consider the relationships of these models to X-ray, EUV, and radio observations, with special emphasis on the X-ray and radio observations, since they describe the impulsive-phase particles more directly. Fig. 5.13 and Table 5.2 give the descriptive parameters of such models. Here we distinguish between "thin-target" and "thick-target" bremsstrahlung (Koch and Motz, 1959) in the following way: if the electrons lose a substantial fraction of their energy to collisions, they radiate in a thick target; in a thin target, they "escape" before doing so. Escape means outward propagation on open field lines that do not connect back to the sun close to the flare site. According to this definition, bremsstrahlung from energetic electrons confined by a magnetic trap having low ambient plasma density will be termed thick target, even though conventionally it is often referred to as thin-target bremsstrahlung.

If the injection of particles into the radiation region occurs continuously, the acceleration mechanism operates throughout the duration of the impulsive burst. If the injection occurs impulsively, the observed X-ray, EUV, and microwave time variation must be due to electron-propagation effects. Viable models include those in which acceleration coincides with the radiation of X-rays and microwaves, as well as those (analogous to the terrestrial aurora) in which the electrons stream some distance before entering the target. Similarly, valid models may envision either bulk heating, which energizes all of the electrons in the acceleration region, or the production of a nonthermal tail that may include only a small fraction of the total electron distribution. We characterize the shape of the electron energy distribution by the terms thermal or nonthermal, referring to whether or not the distribution resembles a Maxwellian.

The models proposed so far can be classified into four classes: (1) thin-target models; (2) thick-target models; (3) partial-precipitation models; and (4) thermal models. In the thin-target, thick-target, and precipitation models the hard X-rays are produced by bremsstrahlung of accelerated electrons with ambient ions, while in the thermal models both electrons and ions are heated to high temperatures and the thermal bremsstrahlung from this hot gas produces hard X-rays. In both cases, the microwave radiation is produced by the electrons through the gyrosynchrotron

MODELS OF IMPULSIVE EMISSION SOURCES

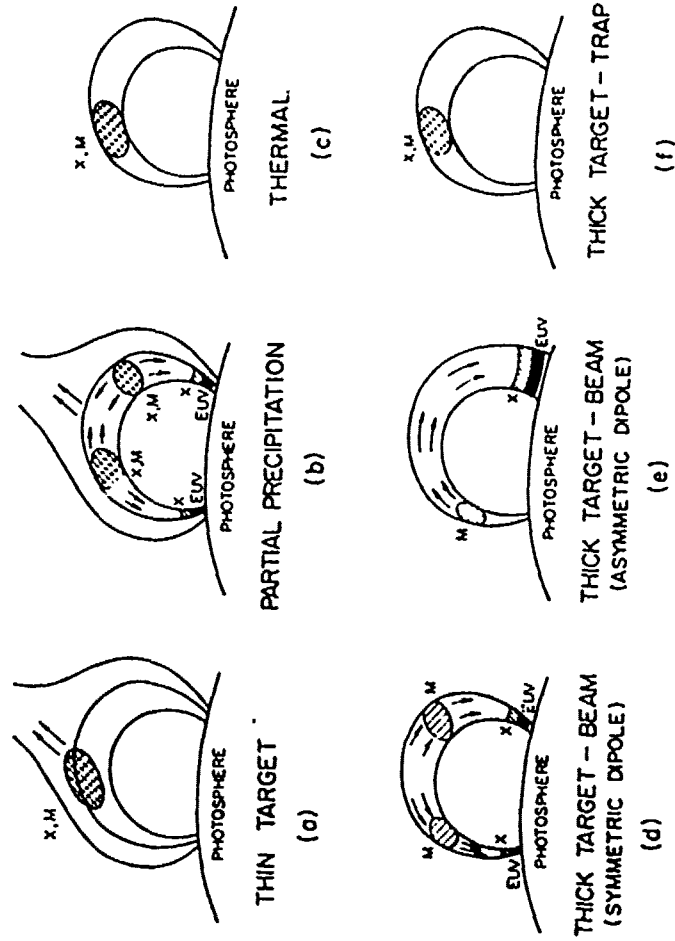


Fig. 5.13 A schematic representation of the thin-target, thick-target, and thermal models of the impulsive emission sources in solar flares. X, M, and EUV represent hard X-ray, microwave, and EUV sources respectively. The arrows indicate directions of propagation for energetic electrons (Kunt, 1979).

TABLE 5.2
A QUALITATIVE ANALYSIS OF THE MODELS OF IMPULSIVE PHASE

Quantity	Type of Model											
	Thin Target		Thick Target Trap		Beam		Partial Precipitation Region 1		Region 2 Turbulent Trap		Thermal Adiabatic Compression	
	Type 1	Type 2	Type 1	Type 2	Type 1	Type 2	Type 1	Type 2	Type 1	Type 2	Type 1	Type 2
Target Ion Density	low	low	low	high	high	high	high	high	low	low	arb	low
Electrons ≥ 10 keV:												
Injection/Acceleration	cont.	imp	negl	cont	negl	cont	cont	cont	small	cont	cont	cont
Escape	large	negl	negl	negl	negl	high	high	negl	low	negl	negl	negl
Beaming	some	negl	negl	high	high	high	high	some	low	negl	negl	negl
Precipitation	negl	th/nth	th/nth	luth	luth	high	high	high	low	negl	negl	th
Spectrum	nth					nth	nth	nth	nth	nth	th	th
Hard X-Rays:												
Polarization	low	negl	negl	negl	negl	high	high	some	low	low	low	negl
Directivity	low	negl	negl	negl	negl	high	high	some	low	low	low	negl
Height of Source	high	high	high	low	low	low	low	low	high	high	arb	high
X-Ray-Microwave												
Source Relationship:												
Temporal	good	good	good	?	?	?	?	poor	good	good	good	good
Spatial	good	good	good	?	?	?	?	poor	good	good	good	good
Peak Flux	good	good	good	?	?	?	?	poor	good	good	good	good
X-ray-EUV Relationship:												
Temporal	poor	poor	poor	?	?	?	?	good	poor	poor	?	?
Spatial	poor	poor	poor	?	?	?	?	good	poor	poor	?	?
Peak Flux	poor	poor	poor	?	?	?	?	good	poor	poor	?	?

Notes: arb = arbitrary cont = continuous imp = impulsive negl = negligible th = thermal nth = nonthermal

mechanism, with self-absorption at longer wavelengths giving rise to a local maximum in the range of 2 to 20 GHz.

The radio and X-ray observations provide the main tests for the various models. The EUV emission provides an additional self-consistency test by requiring a minimum total energy deposited in the upper chromosphere and the transition region. Type III radio bursts, in general, occur during, as well as outside, the times of impulsive phase. However, the intense Type III bursts and/or those extending into the decimetric wavelength range tend to occur primarily during the impulsive phase (Kane, 1975). These Type III bursts, as well as the interplanetary electrons emitted by the sun (presumably, then), must have some relatively direct relationship to the energy release in the impulsive phase (cf. Kane and Lin, 1972).

In the following sections, we discuss the physical properties of various models and the observational constraints on each of them. The models are not complete and self-consistent since they make no attempt to identify the mechanism of particle acceleration or heating. Chapter 4 discusses these questions in detail.

5.8.2. Brief Description of Models

A. Thin-target models. In these models, energetic electrons produce bremsstrahlung X-rays in a region of relatively low ion density ($\leq 10^{10}$ ions cm^{-3}), the time variation of the X-ray emission being a signature of the time variation in the electron acceleration or injection process (Kane and Anderson, 1970; Kane and Lin, 1972; Datiowe and Lin, 1973). The loss of radiating electrons from the source is primarily caused by escape to a much lower density region, where the X-ray emission is negligibly small.

As far as the X-ray bremsstrahlung is concerned, thin-target models use the energetic electrons rather inefficiently and, hence, tend to put more stringent requirements on the electron acceleration process and on the stability of electron propagation against the effects of possible reverse current (Brown and Melrose, 1977). Also, there is no natural explanation of the hard X-ray, EUV relationship in a pure thin-target model. On the other hand, similarity between the hardness of the electron spectra deduced from the X-ray measurements and the spectral hardness of the escaping electrons observed in the interplanetary space is consistent with a substantial fraction of the impulsive hard X-ray emission being produced as thin-target bremsstrahlung. Observations of impulsive hard X-ray bursts from behind-the-limb flares (Kane and Donnelly, 1971; Frost and Dennis, 1971) are also consistent with a thin-target source located at an altitude of $\geq 2 \times 10^4$ km above the photosphere.

B. Thick-target models. In these models, accelerated electrons are injected into a region in which they undergo substantial energy loss during the course of the impulsive event. These are essentially the models described by Kane (1974a) and have many similarities to terrestrial aurora. If the initial injection is into a region of relatively low density, the various models of Fig. 5.13 and Table 5.2 are realized depending on the pitch-angle distribution of the electrons and the relative scale heights, h_e , of the ambient density and, h_b , of magnetic field strength along the loop.

If the pitch angle of electrons is large, or if $h_e \gg h_b$, the result will be the trap models. In the impulsive trapped model, suggested by Takakura and Kai (1966)

(later refined by Takakura and Scalise, 1970; see Takakura, 1974 for review), the time scale for injection of electrons is much shorter than the duration of the impulsive phase of the flare. Historically, this work is the first attempt to tie the microwave and hard X-ray observations together in a self-consistent way. This model predicts gradual hardening of the hard X-ray spectra, even during the decay phase, which is in disagreement with most observations (Kane and Anderson, 1970; Crannell *et al.*, 1978; Elcan, 1978). Bai and Ramaty (1979) have, however, used a model of this type to explain the impulsive bursts in the August 1972 flare.

In the other extreme case, if the electron pitch angle is small and/or $h_e \ll h_b$, the result will be the beamed thick-target model whose X-ray characteristics have been calculated by Syrovatskii and Shmeleva (1971), Brown (1972), Elwert and Haug (1970, 1971), and Petrosian (1973), or a model in which electrons rapidly diffuse from corona to chromosphere (Hudson, 1972, 1973). Since the new electrons rapidly penetrate the higher densities in the solar chromosphere, they lose their energy at a time scale much shorter than the flare duration, so the injection in the model must be continuous. Clearly, in the extreme case of very small pitch angles, little microwave radiation can be produced. In general, characteristics of the microwave flux will depend on details of pitch-angle distribution and field geometry.

The common features of all thick-target models is that the hard X-ray energy yield Y of the electrons is small and varies between 10^{-5} and 10^{-6} , depending on the model and spectrum (for details cf. Petrosian, 1973). If I_x and J_x be, respectively, the total energy flux (erg cm^{-2}) and number flux (photons cm^{-2}) of X-rays $>$ about 20 keV observed at 1 AU, then the total kinetic energy c_e and total number N_e of the accelerated electrons $>$ about 20 keV are given by

$$c_e \approx 2.8 \times 10^{27} \frac{I_x}{Y} \text{ erg} \quad (5.1)$$

$$N_e \approx 2.8 \times 10^{27} \frac{J_x}{Y} \text{ electrons} \quad (5.2)$$

Thus in a "typical" flare with $I_x \sim 10^{-4} \text{ erg cm}^{-2}$ and $J_x \sim 10^3 \text{ photons cm}^{-2}$, there are a total of about 10^{26} electrons with a total kinetic energy of about 10^{29} erg. Such a high energy supplied to the chromosphere (through collisions with ambient electrons) could produce the secondary effects, such as H α , visible continuum, and EUV radiation, the evaporation of hot gas to create the observed soft X-rays, and the formation of coronal transients such as shock waves. Theoretically, acceleration of so many particles and production of such high energies appear to be difficult (Hooyng *et al.*, 1976) unless there is a bulk energization.

In the case of the beamed model, there is also the problem of stability of the electron current beam (Smith, 1975) which can be overcome by a reverse current. As a result, a fraction of the beam energy will be lost due to ohmic heating (Knight and Sturrock, 1977). This fraction will be negligible (and the beam model valid) if the density and temperature of the ambient plasma in the flare region are larger than that of the quiet corona and chromosphere.

Further difficulty with the beam model are the observations of impulsive X-ray bursts from behind-the-limb events (Kane and Donnelly, 1971; Frost and Dennis, 1971; McKenzie, 1975; Roy and Datlowe, 1975). Unless the ambient density in the flux tube along which the beam is directed is considerably higher than that in

the quiet conditions, most of its X-ray radiation will occur deep in the chromosphere, in disagreement with such observations. The beam model is also distinguishable from all other models because of the large degree of polarization and directivity of the resultant X-ray flux. The presently available observations do not have the accuracy and sensitivity necessary to test the models on this basis.

C. Partial-precipitation models. Between the extremes of thin- and thick-target models exist a host of other models that could be classified under the partial-precipitation models. The characteristics of these will depend on the relative importance of the trapped and precipitating electrons. Such models were described qualitatively by Kane (1974a), but a more quantitative analysis has been carried out by Melrose and Brown (1976). Clearly, with the added degree of freedom such models are more flexible. It seems very likely that the dispersion in the observed characteristics of the impulsive phase are caused by variations in the relative importance of the trapped and beamed electrons from one flare to another. Recent studies of the hard X-ray, EUV relationship (Emslie *et al.*, 1978; Donnelly and Kane, 1978; Kane *et al.*, 1978), which indicate that only a small fraction of the total electron energy is sufficient to explain the observed EUV emission, strongly favor the partial-precipitation models.

D. Thermal models. If the initial energy is released in a high-density or turbulent region, so that the "thermalization" time for the energetic particles is much shorter than the duration of the impulsive phase, then a thermal radiation source would result. A significant difference between such thermal and thick-target models is in the X-ray yield. While in the thick-target models the yield is fairly insensitive to the details of the models, in the thermal models the hard X-ray yield depends on the density n and burst duration t

$$Y = \frac{n}{10^{14} \text{ cm}^{-3}} \frac{t}{10 \text{ s}},$$

so that for densities $n > 10^9 \text{ cm}^{-3}$ the yield of a thermal model is larger (and the energy required for production of hard X-rays, smaller) than that of thick-target models.

A low-density, thermal (hard X-ray) model could come about by adiabatic compression (Chubb, 1970) of flare plasma to a high temperature. Mätzler *et al.* (1978) have investigated the implication of the thermal model based on the above analyses. The model includes a common hard X-ray and microwave source, homogeneous and isotropic, with an electron density of $n_e \approx 10^9 \text{ cm}^{-3}$. Mätzler *et al.* find that the adiabatic compression predicts a simple relationship between temperature and the emission measure: $EM \propto T^{3/2}$, which is consistent with their observations (Fig. 5.12), although other observations (Elcan, 1978) do not seem to confirm their findings. The mechanism for compression and the field configuration are not specified, but apparently the model requires a magnetic trap as in the earlier models and an additional confinement mechanism (turbulence?) to keep the electrons in the trap during the compression.

A truly thermal model will require approximately isotropic compression, which is difficult to obtain. Moreover, heating of the plasma before the impulsive phase is required, since if adiabatic compression started at coronal temperatures, the

compression would have to change the volume by an unrealistic factor of 10^4 . An additional difficulty with thermal models may lie in the explanation of the post-burst phenomenon.

5.8.3. Comparison of Models with Observations

A number of observational tests can be applied to the models described above. In terms of the observed radiation or phenomena we can look for the following characteristics associated with each model.

- A. X-rays: yield, spectrum, polarization, directivity, time variation, spatial distribution.
- B. Microwave: same as A.
- C. Other radiation: Type III bursts, white-light continuum, H α , EUV, soft X-rays.
- D. Other effects: shock waves, coronal transients, chromospheric rarefaction, escaping electrons.

The observations made so far are inadequate to fully support or rule out any one model. This is particularly true about the observations that require high spatial and spectral resolution simultaneously with a high time resolution. The following discussion should therefore be primarily regarded as an aid to determine the future observational and theoretical efforts.

A. Hard X-rays. The difference between the X-ray yields of the various models has been described above. There are no high spatial-resolution observations of hard X-rays. We therefore consider here the spectrum, polarization, directivity, and time evolution.

The hard X-ray spectrum gives the most direct information about the spectrum of the high-energy electrons. In simple, homogeneous models a power-law (exponential) X-ray spectrum is obtained from a power-law (thermal) electron spectrum. Existence of hard X-rays with "convex" spectra (Kane and Anderson, 1970; Hoyng *et al.*, 1976; Elcan, 1978; Crannell *et al.*, 1978) has been used as evidence for thermal models. Unfortunately, such simple interpretations are not warranted by the existing observations because they have very poor spectral resolution and no spatial resolution. The latter is very important since, in principle, any observed spectrum can be fit to a multitemperature thermal model or a nonthermal thick-target model with various breaks in the electron spectrum. (The terrestrial aurorae produce convex, hard X-ray spectra from a purely nonthermal electron distribution.)

Strong polarization and directivity effects are expected only in the case of beamed electrons (Brown, 1973; Langer and Petrosian, 1977). At large pitch angles, characteristic of radio-emitting electrons, both of these effects wash out. Thermal and partial-precipitation models have no intrinsic polarization or directivity. Indirect propagation (albedo) reduces these effects in beamed models and introduces a very small residual polarization in isotropic emitting models (Henoux, 1975; Langer and Petrosian, 1977).

The most recent X-ray polarization measurements have not found anything at a level expected from the beaming models, but, due to poor coverage and the

difficulty of making the measurements, the results are not definitive. The center-to-limb variation of the frequency of occurrence (Kane, 1974a; Datlowe *et al.*, 1977) also does not provide a clear support for beamed electrons, although the center-to-limb variation of the X-ray spectral index is not inconsistent with such models.

There has been inadequate analysis of time evolution of fluxes, but the results deserve mention. First of all, there have been various analyses indicating quasi-periodic modulation of X-ray and microwave fluxes (Parks and Winckler, 1971; Frost, 1969; Brown and Hoyng, 1975; Lippa, 1978), the significance of which remains uncertain because of lack of spatial resolution. It seems likely that this modulation arises from successive brightening of separate regions in the flare. The idea of adiabatic compression was motivated by an observed correlation of rise and fall times of single-spike impulsive bursts and the correlation between the X-ray flux and spectral index (Crannell *et al.*, 1978; Mätzler *et al.*, 1978). However, further observations are needed for confirmation of such correlations. In any case, such correlations are neither necessary for (nor unique to) the adiabatic compression model. For example, the time variation of the X-ray spectrum observed during the 4 and 7 August 1972 flares (Hoyng *et al.*, 1976; Ben 1977) has been interpreted by Bai and Ramaty (1978) in terms of a nonthick-target, trap model, where the density ($\sim 3 \times 10^{10} \text{ cm}^{-3}$) is substantially higher than that in the model by Mätzler *et al.*

B. Microwaves. The interpretation of microwave observations is more complicated than the X-rays because (i) the magnetic field strength and geometry play as significant a role as the electron distribution in the production of the microwave fluxes (Takakura, 1973; Mätzler, 1976); and (ii) the microwave, at lower frequencies, are subject to various absorption and suppression processes (Ramaty and Petrosian, 1972). Most calculations of the microwave flux expected from various models have been limited to uniform field geometries. This clearly is unrealistic, and even the high spatial-resolution microwave observations by Kundu and Alissandrakis (1977) demand inhomogeneous field structure. However, with the added free parameters, most probably all of the models become sufficiently flexible to permit close matching with observations (spectrum, polarization, directivity, yield), but no such detailed analyses have been carried out for most of the models.

High spatial-resolution observations have the potential of providing a good test of the models. For example, with such observations one may be able to separate the trapped and precipitating components of the partial-precipitation models.

C. Other radiation and effects. One main strength of the thick-target model lies in its convenience for supplying secondary radiation and effects through the collisional losses of the energetic electrons. These effects include the white-light continuum (Hudson, 1972, 1973), EUV radiation (Kane and Donnelly, 1971) and "chromospheric rarefaction" (Neupert, 1968; Brown, 1973; Hudson and Ohki, 1972), and the simulation of shock waves (Lin and Hudson, 1976). Kane and Donnelly (1971) observed a strong longitude dependence of EUV to hard X-ray flux ratio that places most collisional losses relatively deep in the solar atmosphere, especially for near 20 keV electrons (Donnelly and Kane, 1978). Recent studies (Brown *et al.*, 1978; Emslie *et al.*, 1978; Donnelly and Kane, 1978)

have argued that a beamed thick-target model will produce too much energy deposition and hence much more H α line and EUV emissions than are actually observed. No predictions have been made in regard to these phenomena in thermal models. Explanation of the close temporal relationship between hard X-ray and EUV emissions could turn out to be a major difficulty for the thermal models.

5.9 SOME ANSWERS TO KEY QUESTIONS

We now attempt to answer the three key questions formulated in Section 5.2.

1. Although the temporal relationship between different kinds of emissions is now fairly well established, the interpretation of that relationship in terms of a physical model of the impulsive phase is far from clear. Inadequate spatial and spectral resolution and the absence of good measurements of polarization and directivity of the hard X-ray emission cause large ambiguity in the deduced energy distribution of the energetic electrons. This makes the estimates of the total energy and number of the energetic electrons depend critically on the assumed model of the hard X-ray source. The present observations are therefore unable to answer unambiguously whether the electron distribution is thermal or nonthermal.

2. Before we can analyze the observations, we have to assume the nature of the electron distribution. If we assume that the electron distribution is nonthermal (e.g., a power law), then it invariably turns out that the total energy of electrons $>$ about 20 keV deduced from the impulsive hard X-ray observations is comparable to, or greater than, the total energy required for the post-impulsive-phase phenomena, such as thermal soft X-ray emission, mass motions, particle acceleration, etc. This in turn requires that the energy conversion into accelerated particles be \sim 100% efficient. On the other hand, if we assume that the electron distribution is thermal, then the total energy of the electrons deduced from the impulsive hard X-ray observation is substantially less than the total energy required for the gradual phase. The energy conversion efficiency implied in this case is accordingly smaller. Thus, it is not possible at this time to state unambiguously whether the energetic particles (electrons) produced during the impulsive phase provide the energy necessary for most of the flare. It is fairly certain, however, that these electrons have enough energy to produce all the impulsive-phase emissions. Also energy release, at a lower rate, probably occurs both before and after the impulsive phase.

3. Since the distribution and total energy of the energetic electrons accelerated during the impulsive phase are not unambiguously known, it is not surprising that many different models claim to provide an accurate description of the impulsive phase. The two key parameters, viz. the efficiency and time constant of the acceleration process, are not known at the present time. The time constant is not known because of the inadequate time resolution of the hard X-ray observations. A review of the impulsive hard X-ray and Type III radio-burst data suggests that the basic time constant of the electron acceleration process could be less than or about equal to 0.1 s. In \sim 30% of all impulsive flares, a small fraction of the energetic electrons escape into the outer corona. When these characteristics are combined with the hard X-ray, EUV relationship and the "embedded" nature of

the impulsive EUV sources, it appears that models permitting at least partial precipitation of electrons are to be preferred. Models involving acceleration of electrons at small pitch angles inside a closed magnetic loop that permits free movement of electrons along the field lines but inhibits the electron escape from the loop almost completely are not likely to represent the true characteristics of the impulsive phase. Similar comments apply to models involving adiabatic compression. The existence of several point sources inside the main emission region and the successive brightening of the different point sources, as indicated by radio, optical, and EUV observations, suggests a filamentary structure in the electron acceleration/propagation region.

5.10 FUTURE WORK

It is clear from the discussion in the preceding sections that our understanding of the impulsive phase has increased substantially during the last decade, especially with regard to the quantitative interrelationship between the different impulsive-phase emissions. Although the Skylab observations could not contribute directly to this progress, the Skylab program did encourage new work and new approaches in the studies of this phenomenon. A great deal, however, remains to be done. We give below some of the observations and theoretical studies that must be pursued during the coming years.

5.10.1. Future Observations

In view of the rapid time variations and probably very small spatial extent of the radiating sources present during the impulsive phase, high temporal (\leq about 0.1 s) and spatial (~ 1 arcsec) resolution should be emphasized in all future measurements. The other parameter to be emphasized is high spectral resolution so that basic parameters such as velocities and temperatures in emission sources can be deduced.

In the EUV, UV, optical, and radio wavelength regions, high spatial and spectral resolutions are currently available, or soon will be. The principal aim in these wavelength regions is therefore to achieve a high time resolution (≤ 0.1 s).

On the other hand, the hard X-ray measurements have suffered from the lack of spatial resolution and also poor spectral resolution. Even the time resolution of the past measurements, which was often about or > 1 s, was adequate only to identify the impulsive phase. Good, hard X-ray measurements are particularly important because they are used to deduce the basic quantities, such as total number, energy, and distribution of the energetic electrons. Most current models of the impulsive phase utilize the energetic electrons to provide the necessary energy to the impulsive X-ray, EUV, UV, optical, and radio emission sources and even attempt to provide the energy required for the entire solar flare. Thus, adequate tests of the different models are not possible until satisfactory hard X-ray measurements are available. Specifically at photon energies ≥ 20 keV, the X-ray spectrum (resolution ~ 1 keV) and polarization (sensitivity $\sim 0.1\%$) need to be measured with a spatial resolution of ~ 1 arcsec and a time resolution of ≤ 0.1 s. In addition, observations of the directivity of the X-ray emission made simultaneously

with two or more spacecraft separated widely in solar longitude and having a sensitivity of about 1% and time resolution of a second are required to test the presence of electron beams in the X-ray source.

If there is one lesson to be learned from past experience, it is not to push observations of one wavelength range at the cost of the other. Our hope of solving the impulsive-phase problem lies in a coherent program of observations at a wide range of wavelengths made with a comparable spatial and temporal resolution.

5.10.2. *Future Theoretical Work*

The basic need in all of the viable models of the impulsive phase (those in Table 5.2) lies in realistic numerical modeling and comparison with observations. Some work is already in progress (cf. Smith and Lilliequist, 1978). At present, the microwave data provide the most interesting information and have the smallest degree of model exploitation. Only the impulsive-trap model (Takakura and Kai, 1966) has received a thorough analysis.

Several important related effects have not been studied in any detailed model: the generation of Type II bursts, the production of coronal transient and interplanetary shock waves, and the relationship between the soft and hard X-ray sources. Much of this work probably awaits the present development of elaborate computer models that include enough physics to be realistic; this work is complicated, but probably feasible.

ACKNOWLEDGEMENTS

We wish to acknowledge discussions with T. Bai who was a Consultant for the Impulsive Phase Team. The preparation of this report by S. R. Kane was supported by the National Aeronautics and Space Administration under contract NASS-22307.

REFERENCES

- Alissandrakis, C. E. and Kundu, M. R.: 1975, *Solar Phys.* 41, 119.
- Alissandrakis, C. E. and Kundu, M. R.: 1978, *Astrophys. J.* (in press).
- Anderson, K. A. and Mahoney, W. A.: 1974, *Solar Phys.* 35, 419.
- Anderson, K. A. and Winckler, J. R.: 1962, *J. Geophys. Res.* 67, 4103.
- Arnoldy, R. L., Kane, S. R., and Winckler, J. R.: 1968, *Astrophys. J.* 151, 711.
- Bai, T.: 1977, Ph.D. Thesis, University of Maryland (GSFC preprint X-660-77-85).
- Bai, T. and Ramaty, R.: 1976, *Solar Phys.* 49, 343.
- Bai, T. and Ramaty, R.: 1978, *Astrophys. J.* 219, 705.
- Bai, T. and Ramaty, R.: 1979, *Astrophys. J.* (in press).
- Benz, A. O.: 1977, *Astrophys. J.* 211, 270.
- Brini, R., Evangelisti, F., Fuligni di Grande, M. I., Pizzichini, G., Spizzichino, A., and Vespignani, G. R.: 1973, *Astron. and Astrophys.* 25, 17.
- Brown, J. C.: 1972, *Solar Phys.* 25, 158.
- Brown, J. C.: 1973, *Solar Phys.* 31, 143.
- Brown, J. C.: 1978, preprint.
- Brown, J. C., Canfield, R. C., and Robertson, M. N.: 1978, *Solar Phys.* 57, 399.
- Brown, J. C. and Hoyng, P.: 1975, *Astrophys. J.* 200, 734.
- Brown, J. C. and Melrose, D. B.: 1977, *Solar Phys.* 52, 117.
- Canfield, R. C.: 1974, *Solar Phys.* 34, 339.
- Chubb, I. A.: 1970, in E. R. Dyer (ed.), *Solar-Terrestrial Physics I: Part I*, D. Reidel Publ. Co., Dordrecht, Holland, p. 99.
- Chupp, E. L., Forrest, D. J., and Suri, A. N.: 1975, in S. R. Kane (ed.), 'Solar γ -, X-, and EUV Radiation', *IAU Symp.* 68, 341.
- Cline, T. L., Holt, S. S., and Hones, E. W.: 1968, *J. Geophys. Res.* 73, 431.
- Crannell, C. J., Frost, K. J., Mätzler, C., Ohki, K., and Saba, J. L.: 1978, *Astrophys. J.* 223, 620.
- Datlowe, D. W.: 1975, in S. R. Kane (ed.), 'Solar γ -, X-, and EUV Radiation', *IAU Symp.* 68, 191.
- Datlowe, D. W., Elcan, M. J., and Hudson, H. S.: 1974, *Solar Phys.* 39, 155.
- Datlowe, D. W., Elcan, M. J., Hudson, H. S., and Peterson, L. E.: 1979, in preparation.
- Datlowe, D. W. and Lin, R. P.: 1973, *Solar Phys.* 32, 159.
- Datlowe, D. W., O'Dell, S. L., Peterson, L. E., and Elcan, M. J.: 1977, *Astrophys. J.* 212, 561.
- De Mastus, H. L., and Stover, R.: 1967, *Publ. Astron. Soc. Pacific* 79, 615.
- Donnelly, R. F.: 1968, *Solar Phys.* 5, 123.
- Donnelly, R. F.: 1973, in R. Ramaty and R. G. Stone (eds.), *High Energy Phenomena on the Sun*, NASA SP-342, p. 242.
- Donnelly, R. F. and Kane, S. R.: 1978, *Astrophys. J.* 222, 1043.
- Donnelly, R. F., Wood, A. T., Jr., and Noyes, R. W.: 1973, *Solar Phys.* 29, 107.
- Elcan, M. J.: 1978, *Astrophys. J. Letters* 226, L99.
- Elwert, C. and Haug, E.: 1970, *Solar Phys.* 15, 234.
- Elwert, G. and Haug, E.: 1971, *Solar Phys.* 20, 413.
- Emslie, A. G., Brown, J. C., and Donnelly, R. F.: 1978, *Solar Phys.* (in press).
- Emslie, A. G. and Noyes, R. W.: 1978, *Solar Phys.* 57, 373.
- Enome, S., Kakinuma, T., and Tanaka, H.: 1969, *Solar Phys.* 6, 428.
- Enome, S. and Tanaka, H.: 1973, in R. Ramaty and R. G. Stone (eds.), *High Energy Phenomena on the Sun*, NASA SP-342, p. 78.
- Frost, K. H.: 1964, in W. Hess (ed.) *AAS-NASA Symposium on the Physics of Solar Flares*, NASA SP-50, p. 139.
- Frost, K. J.: 1969, *Astrophys. J. Letters* 158, 1159.
- Frost, K. J. and Dennis, B. R.: 1971, *Astrophys. J.* 165, 655.
- Grineva, Yu. I., Karev, V. I., Korneev, V. V., Krutov, V. V., Mandelstam, S. L., Vainstein, L. A., Valiliev, B. N., and Zhitnik, I. A.: 1973, *Solar Phys.* 29, 441.

- Gandice, C. and Castelli, J.: 1973, in R. Ramaty and R. G. Stone (eds.), *High Energy Phenomena on the Sun*, NASA SP-342, p. 87.
- Hall, L. A.: 1971, *Solar Phys.* 21, 167.
- Hall, L. A. and Hinteregger, H. E.: 1969, in C. de Jager and Z. Švestka (eds.), *Solar Flares and Space Research*, North Holl. Publ. Co., Amsterdam, p. 81.
- Henoux, J. C.: 1975, *Solar Phys.* 42, 219.
- Hobbs, R. W., Jordan, S. D., Maran, S. P., Caul, H. M., and Webster, W. J., Jr.: 1973, *Astrophys. Letters* 15, 193.
- Holt, S. S. and Ramaty, R.: 1969, *Solar Phys.* 8, 119.
- Hoyng, P., Brown, J. C., and Van Beek, H. I.: 1976, *Solar Phys.* 48, 197.
- Hudson, H. S.: 1972, *Solar Phys.* 24, 414.
- Hudson, H. S.: 1973, in R. Ramaty and R. G. Stone (eds.), *High Energy Phenomena on the Sun*, NASA SP-342, p. 207.
- Hudson, H. S.: 1978, *Astrophys. J.*, 224, 235.
- Hudson, H. S., Canfield, R. C., and Kane, S. R.: 1978, *Solar Phys.* (in press).
- Hudson, H. S. and Ohki, K.-I.: 1972, *Solar Phys.* 23, 155.
- Hudson, H. S., Peterson, L. L., and Schwartz, D. A.: 1969, *Astrophys. J.* 157, 389.
- Hurley, K. and Duprat, G.: 1977, *Solar Phys.* 52, 107.
- Jager, C. de: 1967, *Solar Phys.* 2, 327.
- Jager, C. de; and Kundu, M. R.: 1963, in W. Priestu (ed.), *Space Research 3*, North Holl. Publ. Co., Amsterdam p. 836.
- Jager, C. de and de Jonge, G.: 1978, *Solar Phys.* 58, 127.
- Jenssens, R. J. and White, K. P., III: 1976, *Solar Phys.* 11, 299.
- Kahler, S. W.: 1975, in S. R. Kane (ed.), 'Solar, Gamma X, and EUV Radiation', *IAU Symp.* 68, 211.
- Kahler, S. W. and Kreplin, R. W.: 1971, *Astrophys. J.* 168, 531.
- Kahler, S. W., Petraso, R. D., and Kane, S. R.: 1976, *Solar Phys.* 50, 179.
- Kane, S. R.: 1969, *Astrophys. J. Letters* 157, L139.
- Kane, S. R.: 1971, *Astrophys. J.* 170, 587.
- Kane, S. R.: 1972a, *Solar Phys.* 27, 174.
- Kane, S. R.: 1972b, *Space Sci. Rev.* 13, 822.
- Kane, S. R.: 1973, in R. Ramaty and R. G. Stone (eds.), *High Energy Phenomena on the Sun*, NASA SP-342, p. 55.
- Kane, S. R.: 1974a, in G. Newkirk, Jr. (ed.), 'Coronal Disturbances', *IAU Symp.* 57, 105.
- Kane, S. R.: 1974b, *Bull. Am. Astron. Soc.* 6, 289.
- Kane, S. R.: 1975, *Bull. Am. Astron. Soc.* 7, 352.
- Kane, S. R.: 1979 (in preparation).
- Kane, S. R. and Anderson, K. A.: 1970, *Astrophys. J.* 162, 1003.
- Kane, S. R. and Anderson, K. A.: 1976, Paper No. 5518, presented at Fall A. G. U. Meeting, San Francisco.
- Kane, S. R. and Donnelly, R. F.: 1971, *Astrophys. J.* 164, 151.
- Kane, S. R., Frost, K. J., and Donnelly, R. F.: 1978, presented XX1st COSPAR Meeting, 29 May - 10 June, Innsbruck. Also 1979, *Astrophys. J.* 234 (in press).
- Kane, S. R. and Lin, R. P.: 1972, *Solar Phys.* 23, 457.
- Kelly, P. I. and Rense, W. A.: 1972, *Solar Phys.* 26, 431.
- Knight, J. W. and Sturrock, P. A.: 1977, *Astrophys. J.* 218, 306.
- Koch, H. W. and Motz, J. W.: 1959, *Rev. Mod. Phys.* 31, 920.
- Korchak, A. A.: 1971, *Solar Phys.* 18, 284.
- Kundu, M. R.: 1959, *Ann d'Astrophys.* 22, 1.
- Kundu, M. R.: 1961, *J. Geophys. Res.* 66, 4308.
- Kundu, M. R.: 1965, *Solar Radio Astronomy*, Intersec. Publ., N. Y.
- Kundu, M. R. and Athsandrakis, C. L.: 1977, *Bull. Amer. Astron. Soc.* 9, 328.
- Kundu, M. R. and Athsandrakis, C. L., Bregman, J. D. and Hin, A. Z.: 1977, *Astrophys. J.* 213, 278.

REFERENCES

- Kundu, M. R., Alissandrakis, C. E., and Kahler, S. W.: 1976, *Solar Phys.* 50, 429.
- Kundu, M. R. and Liu, S. Y.: 1973, *Solar Phys.* 29, 409.
- Kundu, M. R., Velusamy, T., and Becker, R. H.: 1974, *Solar Phys.* 34, 217.
- Kundu, M. R. and Vlahos, L.: 1978, *Solar Phys.* (in press).
- Langer, S. and Petrosian, V.: 1977, *Astrophys. J.* 216.
- Lin, R. P.: 1970, 'Acceleration of 10-100 keV electrons in solar flares', presented at the Seminar on the Acceleration of Particles in Near Earth and Interplanetary Space, Galaxy, and Metagalaxy, Leningrad, U.S.S.R., July 13-15.
- Lin, R. P.: 1973, in R. Ramaty and R. G. Stone (eds.), *High Energy Phenomena on the Sun*, NASA SP-342, p. 439.
- Lin, R. P.: 1979, (in preparation).
- Lin, R. P. and Hudson, H. S.: 1971, *Solar Phys.* 1, 412.
- Lin, R. P. and Hudson, H. S.: 1976, *Solar Phys.* 50, 153.
- Lippa, B.: 1978, *Solar Phys.* (in press).
- McKenzie, D. L.: 1972, *Astrophys. J.* 175, 481.
- McKenzie, D. L.: 1975, *Solar Phys.* 49, 117.
- Mätzler, C.: 1976, *Solar Phys.* 49, 117.
- Mätzler, C., Bai, T., Crannell, C. J., and Frost, K. J.: 1978, *Astrophys. J.* 223, 1058.
- McLose, D. B. and Brown, J. C.: 1976, *Mon. Not. Roy. Astron. Soc.* 176, 15.
- Nakada, M. P., Neupert, W. M., and Thomas, R. J.: 1974, *Solar Phys.* 37, 429.
- Najita, K. and Orrall, F. Q.: 1970, *Solar Phys.* 15, 176.
- Neidig, D. F.: 1976, Ph.D. Thesis, Pennsylvania State University.
- Neidig, D. F.: 1978, *Solar Phys.* 57, 385.
- Neupert, W. M.: 1968, *Astrophys. J. Letters* 153, L59.
- Neupert, W. M., Thomas, R. J., and Chapman, R. D.: 1974, *Solar Phys.* 34, 349.
- Noyes, R. W.: 1973, in R. Ramaty and R. G. Stone (eds.), *High Energy Phenomena on the Sun*, NASA SP-342, p. 231.
- Ohki, K.: 1969, *Solar Phys.* 1, 260.
- Parks, G. K. and Winckler, J. R.: 1969, *Astrophys. J. Letters* 155, L117.
- Parks, G. K. and Winckler, J. R.: 1971, *Solar Phys.* 16, 186.
- Peterson, L. E., Datlowe, D. W., and McKenzie, D. L.: 1973, in R. Ramaty and R. G. Stone (eds.), *High Energy Phenomena on the Sun*, NASA SP-342, p. 132.
- Peterson, L. E. and Winckler, J. R.: 1959, *J. Geophys. Res.* 64, 697.
- Petrosian, V.: 1973, *Astrophys. J.* 186, 291.
- Phillips, K. J. H.: 1973, *The Observatory*, 93, 17.
- Pinter, S.: 1969, *Solar Phys.* 8, 142.
- Ramaty, R.: 1969, *Astrophys. J.* 158, 753.
- Ramaty, R. and Petrosian, V.: 1972, *Astrophys. J.* 178, 241.
- Roy, J.-R. and Datlowe, D. W.: 1975, *Solar Phys.* 40, 165.
- Rust, D. M., and Hegwer, F.: 1975, *Solar Phys.* 40, 141.
- Rust, D. M., Nakagawa, Y., and Neupert, W. M.: 1975, *Solar Phys.* 41, 397.
- Santangelo, N., Horstman, H., and Horstmann-Moretti, E.: 1973, *Solar Phys.* 29, 143.
- Slonim, Yu. M. and Korobova, Z. B.: 1975, *Solar Phys.* 40, 397.
- Smith, D. F.: 1975, *Astrophys. J.* 201, 521.
- Smith, D. F. and Lilliequist, C. G.: 1978, *Astrophys. J.* (in press).
- Stewart, R. T.: 1978, *Solar Phys.* 58, 121.
- Švestka, Z.: 1970, *Solar Phys.* 13, 471.
- Švestka, Z.: 1976, *Solar Flares*, D. Reidel Publ. Co., Dordrecht, Holland.
- Syrovatskii, S. I. and Shmeleva, O. P.: 1971, Lebedev Institute Preprint, 158.
- Takakura, T.: 1960, *Publ. Astron. Soc. Japan*, 12, 325.
- Takakura, T.: 1972, *Solar Phys.* 26, 151.
- Takakura, T.: 1973, in R. Ramaty and R. G. Stone (eds.), *High Energy Phenomena on the Sun*, NASA SP-342, p. 179.

- Takakura, I.: 1974, in S. R. Kane (ed.), 'Solar Gamma , X , and EUV Radiation', *IAU Symp.* 68, 299.
- Takakura, T. and Kai, K.: 1966, *Publ. Astron. Soc. Japan* 18, 57.
- Takakura, I. and Scalise, E., Jr.: 1970, *Solar Phys.* 11, 434.
- Talon, R., Vedrenne, G., Melioransky, A. S., Pissarenko, N. F., Shamolin, V. M., and Likin, O. B.: 1975, in S. R. Kane (ed.), *Solar Gamma , X , and EUV Radiation*, *IAU Symp.* 68, 315.
- Tanaka, H. and Kakinuma, I.: 1962, *J. Phys. Soc. Japan, Supplement A-11* 17, 211.
- Thomas, R. J. and Neupert, W. M.: 1975, *Bull. Amer. Astron. Soc.*, 7, 355.
- Indo, I. P., Mandelstam, S. L., and Shuryghin, A. I.: 1973, *Solar Phys.* 32, 469.
- Indo, I. P., Shuryghin, A. I., and Stellen, W.: 1976, *Solar Phys.* 46, 219.
- Tomblin, J. I.: 1972, *Astrophys. J.* 171, 377.
- Van Beek, H. J., De Jetter, L. D., and De Jager, C.: 1974, *Space Research XIV*, 447.
- Vorpahl, J.: 1972, *Solar Phys.* 26, 397.
- Vorpahl, J.: 1973, *Solar Phys.* 29, 447.
- Vorpahl, J., Gibson, L. G., Landecker, P. B., McKenzie, D. L., and Underwood, J. H.: 1975, *Solar Phys.* 45, 199.
- Vorpahl, J. and Zirin, H.: 1970, *Solar Phys.* 11, 285.
- Wild, J. P.: 1964, in W. N. Hess (ed.), *Physics of Solar Flares*, NASA SP-503, p. 161.
- Wood, A. T., Jr., Noyes, R. W., Dupree, A. K., Huber, M. C. E., Parkinson, W. H., Reeves, E. M., and Withbroe, G. L.: 1972, *Solar Phys.* 24, 169 and 180.
- Zirin H.: 1978, *Solar Phys.* 58, 95.
- Zirin, H., Pruss, G., and Vorpahl, J.: 1971, *Solar Phys.* 19, 463.
- Zirin, H., and Tanaka, K.: 1973, *Solar Phys.* 32, 173.